All roads lead to Roma...

# *IEEE Ultrasonics Symposium 2009*
## *Rome, Sept. 20-23*

# Short Course 6A: Estimation and Imaging of Blood Flow Velocity

**Hans Torp and Lasse Løvstakken**
Department of Circulation and Medical Imaging
Norwegian University of Science and Technology
Trondheim, Norway

**Web-page:** http://folk.ntnu.no/lovstakk/dopplershortcourse2009
(contains supporting literature and Matlab demonstrations)

**E-mail:** Hans.Torp(at)ntnu.no, Lasse.Lovstakken(at)ntnu.no

**Course summary:** This course provides a basic understanding of the physical principles and signal processing methods for estimation of blood flow velocity. The course begins with an overview of currently used techniques for velocity estimation using pulsed- and continuous-wave Doppler, and color flow imaging. Fundamental challenges related to data acquisition will be presented. Further, statistical models for the received signal as well as commonly used velocity estimators will be developed. The suppression of clutter from slowly moving targets is central to all processing schemes and will be given special attention. Finally, and introduction to advanced topics such as adaptive clutter filtering and 2-D / 3-D vector velocity estimation techniques will be given. Principles and practical limitations will be discussed, and potential clinical applications will be shown.

# Course outline

### Lecture 1 – Basic principles of Doppler ultrasound

- General introduction to course
- Clinical motivation for velocity measurements with ultrasound and a short Doppler history lesson
- CW-Doppler measurements
- Random signal model and spectrum analysis
- PW-Doppler measurements

### Lecture 2 – Color flow imaging

- Clinical motivation and short history lesson
- Data acquisition in CFI
- Mean (axial) velocity estimation in CFI
- Clutter filtering in CFI
- Display techniques in CFI

### Lecture 3 – Advanced topics, trade-offs and limitations

- Limitations of conventional Doppler / CFI techniques
- Patient safety aspects
- Advanced axial velocity estimators
- Adaptive clutter filtering

### Lecture 4 – Future directions

- 2D vector velocity estimation
- High frame rate CFI
- Real-time 3-D CFI

IEEE

UFFC

# Doppler Short Course '09

*Estimation and imaging of blood flow velocity*

*Part I: Basic principles*

**2009 Ultrasonics Symposium, Rome, Italy**
Hans Torp and Lasse Løvstakken
Department of Circulation and Medical Imaging
Norwegian University of Science and Technology

NTNU
Norwegian University of Science and Technology





## Why measure and visualize blood flow?

- Measure blood supply to an organ
- Angiography without contrast agent
- Measure pressure drop through an stenotic valve
- …….

NTNU
Norwegian University of Science and Technology

3

# Course outline

- Lecture 1: Basic Doppler techniques (Torp)
  - Basic principles of Doppler ultrasound
  - PW- and CW-Doppler
- Lecture 2: Color flow imaging (Løvstakken)
  - Data acquisition
  - Velocity estimation
  - Clutter filtering
  - Display techniques
- Lecture 3: Advanced topics (Løvstakken/Torp)
  - Limitations of conventional techniques
  - Patient safety issues
  - Advanced velocity estimators
  - Adaptive clutter filtering
- Lecture 4: Future directions (Løvstakken)
  - Vector-velocity estimation
  - High frame rate imaging
  - Real-time 3-D CFI

NTNU
Norwegian University of Science and Technology



4

# Course objectives

- Review and understanding of basic principles of ultrasound Doppler imaging
- Emphasis on signal models and -processing
- Clinical examples in cardiology and vascular imaging

NTNU
Norwegian University of Science and Technology

5

# Lecture 1 outline

- Principles and applications of continuous-wave (CW) Doppler
- Random signal model and spectrum analysis
- Pulsed-wave (PW) Doppler
- Time shift versus Doppler shift

NTNU
Norwegian University of Science and Technology



6

# Red blood cells are hardly visible in the ultrasound image

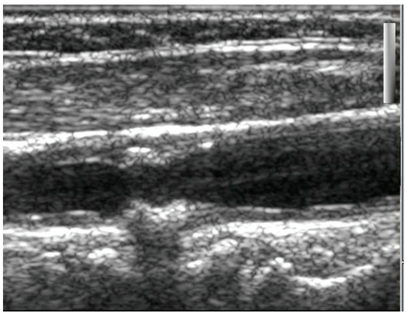

Carotid artery with calcified plaque

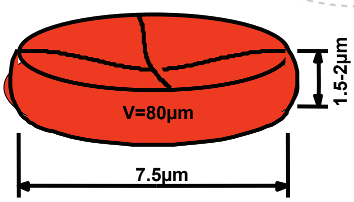


Red blood cell

NTNU
Norwegian University of Science and Technology

7

# High frequency / low acoustic noise → Blood visible

**13 MHz epicardial probe, left ventricle**
**450 frames/sec**

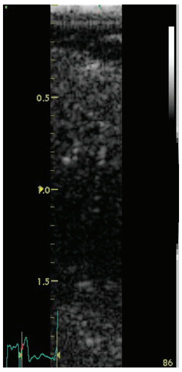

**Real-time**

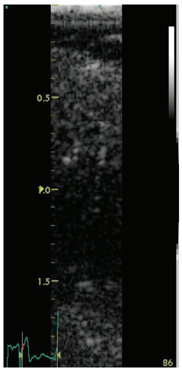

**Slow motion 10%**

High frame-rate required to see the motion

| Blood Velocity | Displacement 50 frames/sec | Minimum Frame rate |
|---|---|---|
| 5 cm/sec | 1 mm | 50 fr/sec |
| 50 cm/sec | 1 cm | 500 fr/sec |
| 5.0 m/sec | 10 cm | 5000 fr/sec |

**For high velocity jet flow,**
**e.g. in heart valve deseases**
**Frame rate ~ 5000 is required**
**to observe and measure velocity**

NTNU
Norwegian University of Science and Technology



8

# The Doppler effect

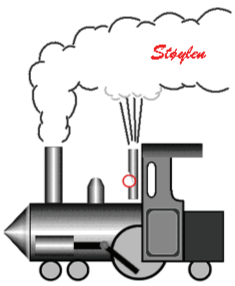

**Christian Andreas Doppler**
**(1803 - 1853)**
**Described the Doppler effect to *light waves***

**Cristoph Ballot**
**demonstrated the Doppler effect for *sound waves (1845)***

***Doppler shift:*** $f_d = f_0 \, v/c$

NTNU
Norwegian University of Science and Technology

9

# Doppler speed control

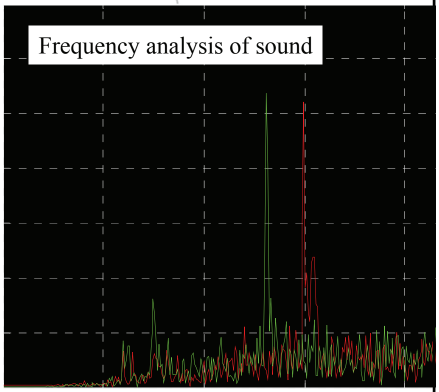


**Frequency before pass by: 130.85 Hz**
**Frequency after pass by: 150.80 Hz**

**Dopplershift: +/- 9.55 Hz ~ +/- 6.8 %**
**Motor bike speed: 340[m/s] * 6.8/100 *3.6 = 83.3 km/h**

**Speed limit = 80 km/h**

NTNU
Norwegian University of Science and Technology



10

# Doppler shift from moving blood

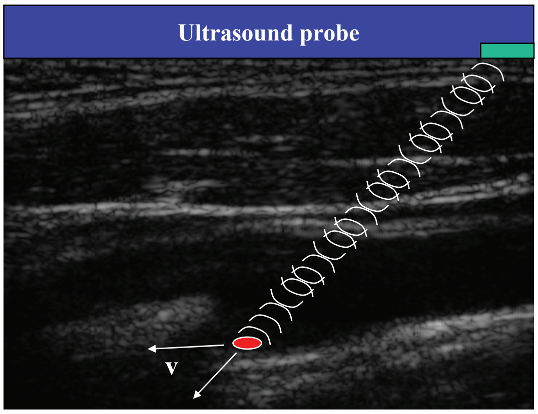


**Dopplershift**
fd = fo v/c
+ fo v/c
= 2 fo v/c

NTNU
Norwegian University of Science and Technology

11

# Continuous wave Doppler

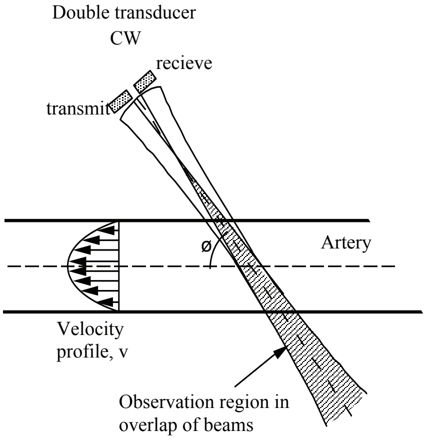


Signal from all scatterers within the ultrasound beam included in the received signal

NTNU
Norwegian University of Science and Technology



12

# Blood velocity calculated from measured Doppler-shift

$$f_d = \frac{2 f_0 v \cos(\theta)}{c}$$

$$v = \frac{c \cdot f_d}{2 f_0 \cos(\theta)}$$

| | |
|---|---|
| $f_d$ : | Dopplershift |
| $f_o$ : | transmitted frequency |
| v : | blood velocity |
| θ : | beam angle |
| c : | speed of sound in blood (1540 m/s ) |

NTNU
Norwegian University of Science and Technology

13

# Signal processing for CW Doppler

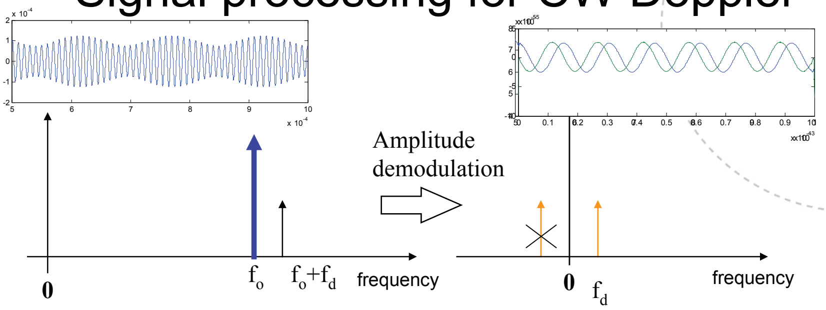


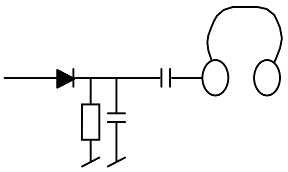

Amplitude demodulation

Satumora, Japan, 1957

Complex Demodulation
Separate positive and negative
Doppler shift

NTNU
Norwegian University of Science and Technology



14

# Doppler blood flow meter (Pedof 1976)

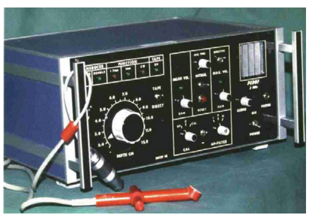

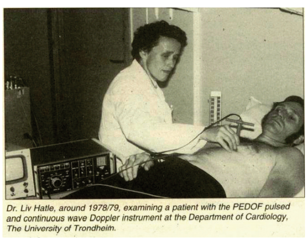


Blood velocity Mitral inflow

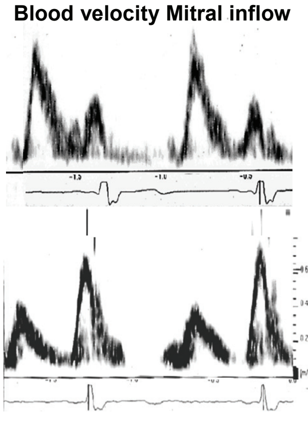

Normal relaxation

Delayed relaxation

NTNU
Norwegian University of Science and Technology

15

# Continuity of flow to assess stenosis

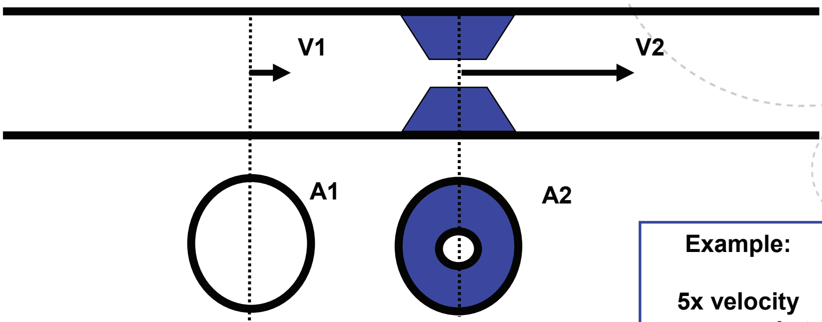


$V1 * A1 = V2 * A2$

% reduction $\dfrac{A1 - A2}{A1} = \dfrac{V2 - V1}{V2}$

**Example:**

**5x velocity corresponds to 80% stenose**

*Area reduction depends only on the velocity V2/V1; independent of diameter and angle*

NTNU
Norwegian University of Science and Technology



16

# Reduction in blood pressure in a stenotic artery

Bernouli's equation describes pressure drop due to increase in kinetic energy

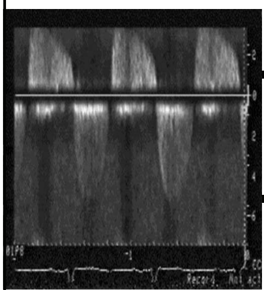

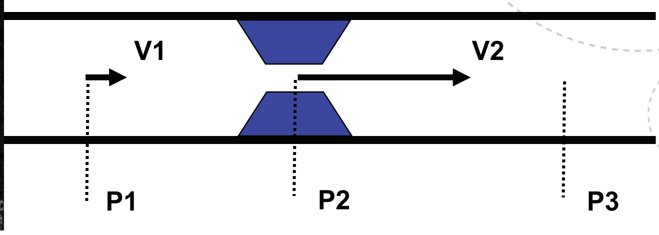


**Pressure drop (gradient) :** $P1 - P3 = 4\,V2^{2}$

**Example**: 80% aortic-stenosis
V1= 1 m/s V2 = 5 m/s pressure-gradient 4*5*5 = 100 mmHg

Normal aortic pressure 120 mmHg corresponds to
220 mmHg ventricular pressure!

NTNU
Norwegian University of Science and Technology

# Aortic stenosis and regurgitation by CW Doppler

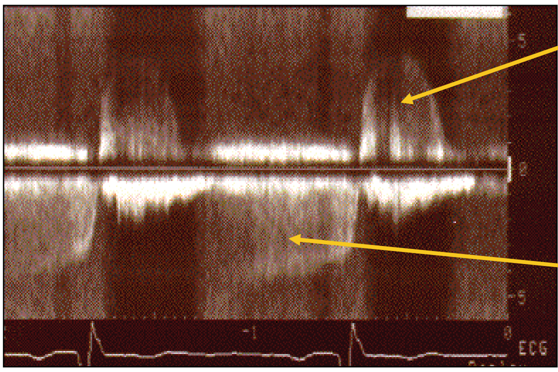


NTNU
Norwegian University of Science and Technology





# Doppler spectrum analysis: Velocities separated in frequency

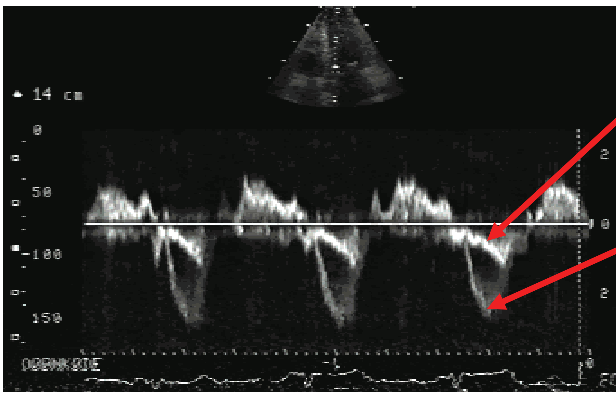


NTNU
Norwegian University of Science and Technology

19

# Lecture 1 outline

- Principles and applications of CW Doppler
- **Random signal model and spectrum analysis**
- Pulsed wave Doppler
- Time shift versus Doppler shift

NTNU
Norwegian University of Science and Technology



20

## Signal from a large number of red blood cells add up to a Gaussian random process

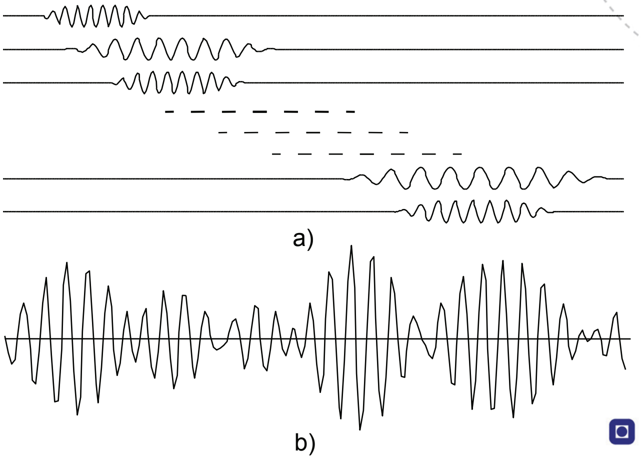


NTNU
Norwegian University of Science and Technology

21

Power spectrum of the Doppler signal represents the distribution of velocities within the blood vessel

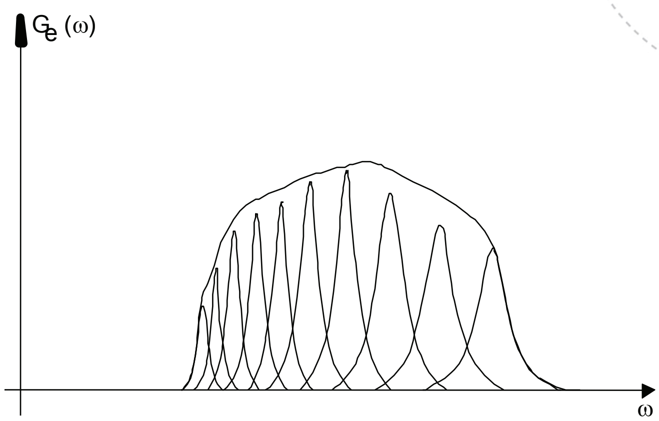


NTNU
Norwegian University of Science and Technology



22

# Doppler spectrum

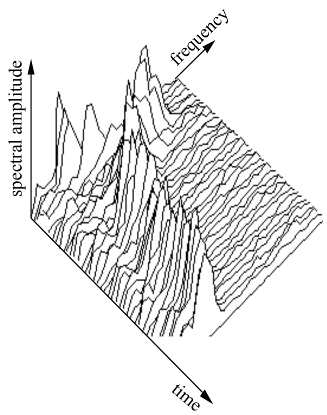


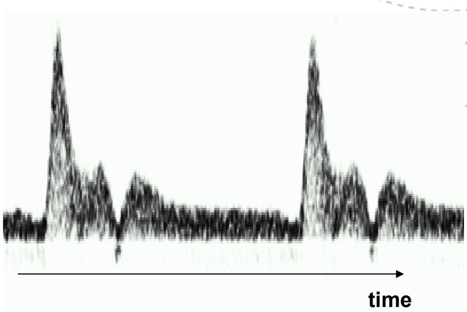


NTNU
Norwegian University of Science and Technology

# Definition of Complex Gaussian process

$$p(z) = \pi^{-N} |\mu|^{-1} e^{-z^T \mu^{-1} z}$$

signal vector $z = z(1), z(2), ..., z(N)$

Covariance matrix $\mu = \langle z^{\mathrm{T}} z \rangle = \{\langle z(k)^* \cdot z(n) \rangle\}_{k,n}$

$\langle - \rangle$ is expected value (ensemble average)

$$Note\ that: \langle z(k) \cdot z(n) \rangle = 0$$

NTNU
Norwegian University of Science and Technology





# Stationary complex Gaussian process

**Autocorrelation function**

$$R(m) \equiv \langle z(n)^* z(n+m) \rangle \quad m = 0, \pm 1, \pm 2, ......$$

**Power spectrum**

$$G(\omega) \equiv \sum_m R(m) e^{-i\omega m} \quad ; \quad -\pi < \omega < \pi$$

**Autocorrelation function = coeficients in Fourier series of G**

$$R(m) = \frac{1}{2\pi} \int_{-\pi}^{\pi} d\omega G(\omega) e^{i\omega m}$$

NTNU
Norwegian University of Science and Technology

# Power spectrum estimate
# Statistical properties

**Power spectrum estimate:**

$$G_N(\omega) = \frac{1}{N}\left|Z_N(\omega)\right|^2 \qquad Z_N(\omega) = \sum_{m=-\infty}^{\infty} w_N(m) z(m) e^{-i\omega m}$$

**Expected value:**

$$< G_N(\omega) >= \frac{1}{2\pi}\int_{-\pi}^{\pi} d\lambda \left|W(\lambda)\right|^2 G(\omega-\lambda) \qquad W(\omega) = \sum_m w_N(m) e^{-i\omega m}$$

NTNU
Norwegian University of Science and Technology





# Power spectrum estimate
# Statistical properties

**Covariance:**

$$\operatorname{cov}\left(G_N(\omega), G_N(\omega+\Delta)\right) = \left|\frac{1}{2\pi N}\int_{-\pi}^{\pi} d\lambda W(\lambda) W^*(\lambda-\Delta) G(\omega-\lambda-\Delta)\right|^2$$

$$= \begin{cases} < G_N(\omega) >^2 & \text{when } \Delta = 0 \\ 0 & \text{when } |\Delta| > 1/N \end{cases}$$

**Exponential probability density distribution**
**Fractional variance = 100%**

NTNU
Norwegian University of Science and Technology

27

# Clutter noise in spectral Doppler

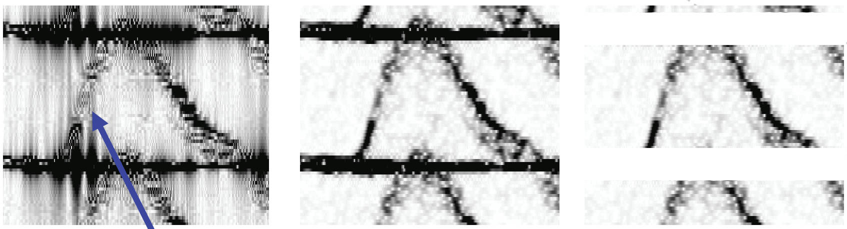

**Rectangular window** **Hamming window** **High pass filter**

Interfering sidelobes from clutter signal

NTNU
Norwegian University of Science and Technology



28

# Frequency resolution versus temporal resolution

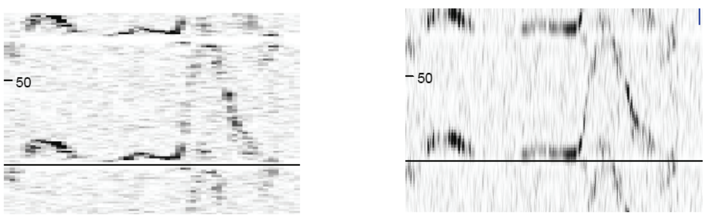


**Window length 64** **Window length 16**

Time-bandwidth product: $\Delta f_d * \Delta T = 1$

NTNU
Norwegian University of Science and Technology

# Properties of power spectrum estimate

- Fractional variance = 1 independent of the window form and size
- $G_N(\omega 1)$ and $G_N(\omega 2)$ are uncorrelated when $|\omega 1-\omega 2| > 1/N$
- Increasing window length N gives better frequency resolution, but no decrease in variance
- Smooth window functions give lower side lobe level, but wider main lobe than the rectangular window
- Decrease in variance can be obtained by averaging spectral estimates from different data segments.

NTNU
Norwegian University of Science and Technology





# Lecture 1 outline

- Principles and applications of CW Doppler
- Random signal model and spectrum analysis
- **Pulsed wave Doppler**
- Time shift versus Doppler shift

NTNU
Norwegian University of Science and Technology

# Continous Wave Doppler → Pulsed Wave Doppler

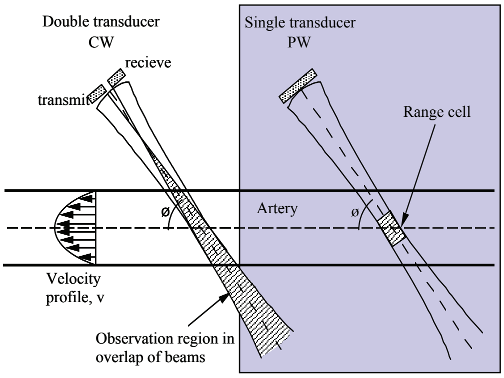


Sample volume length = cT/2

T = pulse length

Signal from all scatterers within the ultrasound beam

Signal from a limited sample volume

Satumora, Japan, 1957

Perroneau, Baker, Wells 1967-69

NTNU
Norwegian University of Science and Technology





# 2D signal model PW Doppler

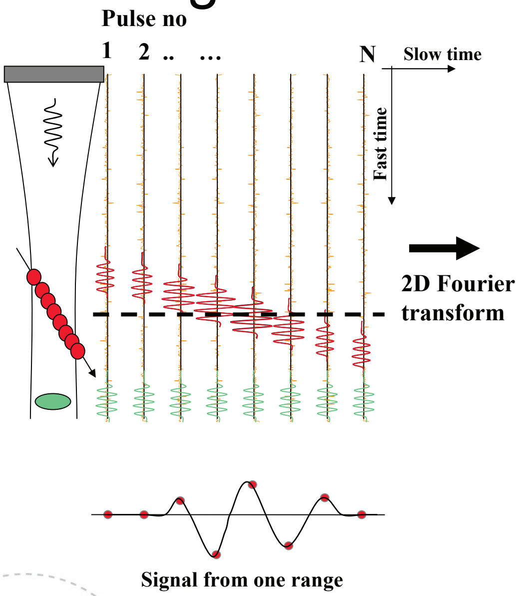


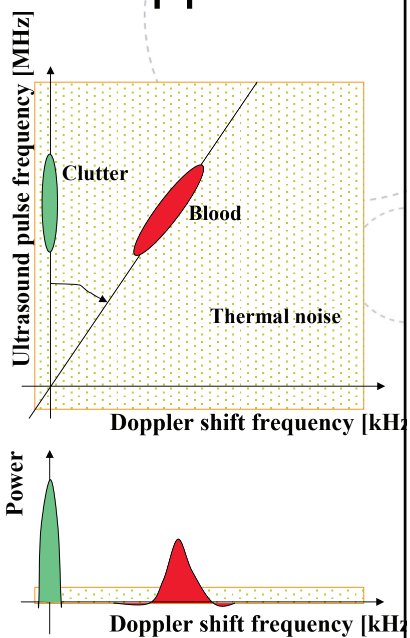

33

# 2D signal model RF versus base band

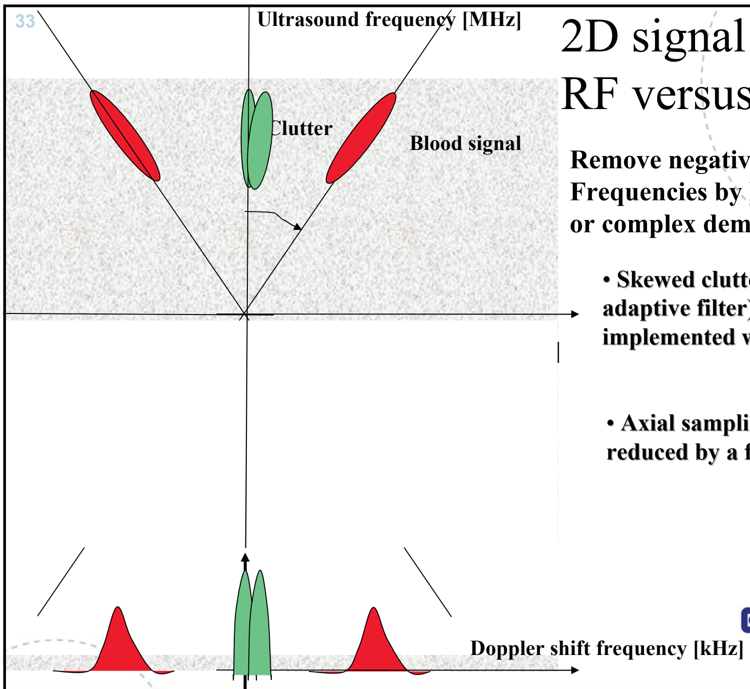


**Remove negative ultrasound Frequencies by Hilbert transform or complex demodulation**

- **Skewed clutter filter (signal adaptive filter) can be implemented with 1D filtering**
- **Axial sampling frequency reduced by a factor > 4**

NTNU
Norwegian University of Science and Technology



34

# Aliasing in PW Doppler

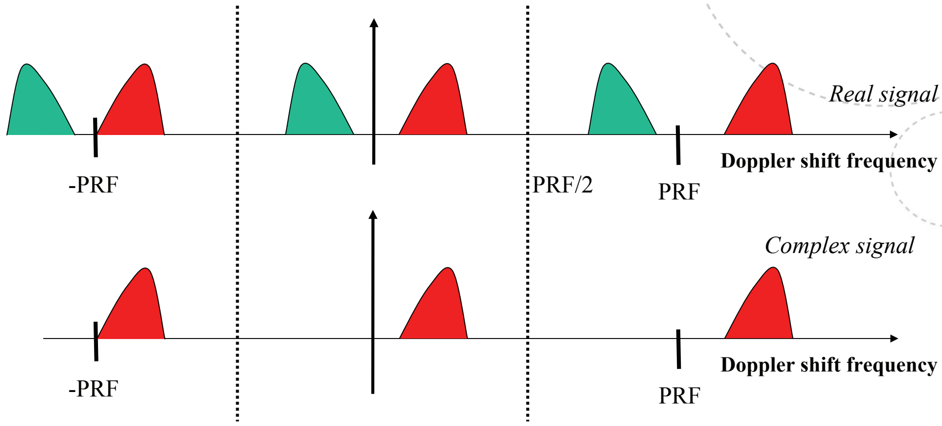


NTNU
Norwegian University of Science and Technology

35

# Aliasing in PW Doppler

Example: Subclavian Artery

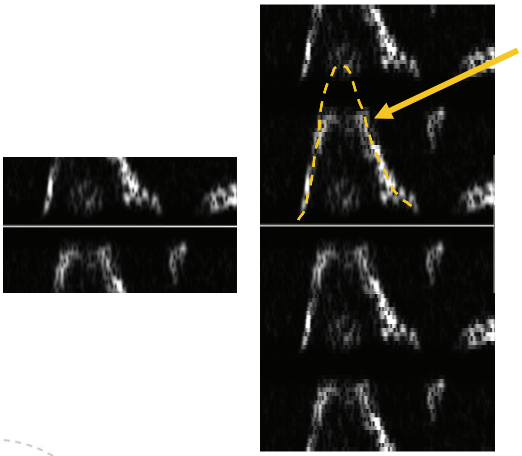

Velocity waveform restored by stacking

NTNU
Norwegian University of Science and Technology



36

# Aliasing PW versus CW Doppler

Example: Aourtic valve leakage jet

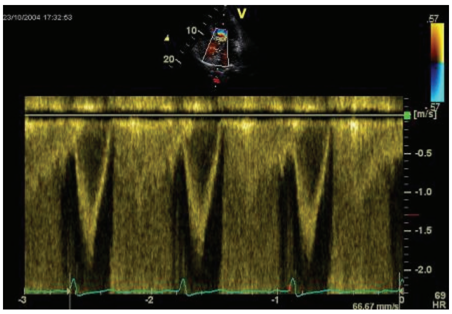

PW Doppler

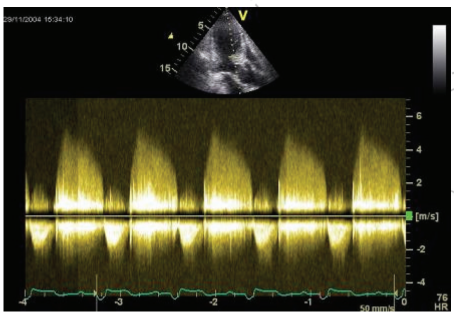

CW Doppler

NTNU
Norwegian University of Science and Technology

# Summary PW Doppler

- Complex demodulation give direction information of blood flow
- PW Doppler suffers from aliasing in many cardiac applications
- Aliasing can be restored by baseline shift, or stacking, if bandwidth is limited

NTNU
Norwegian University of Science and Technology





# Lecture 1 outline

- Principles and applications of CW Doppler
- Random signal model and spectrum analysis
- Pulsed wave Doppler
- **Time shift versus Doppler shift**

NTNU
Norwegian University of Science and Technology

39

# Is Pulsed wave Doppler based on Doppler shift or time shift?

94 *Ultrasound's interaction with blood*

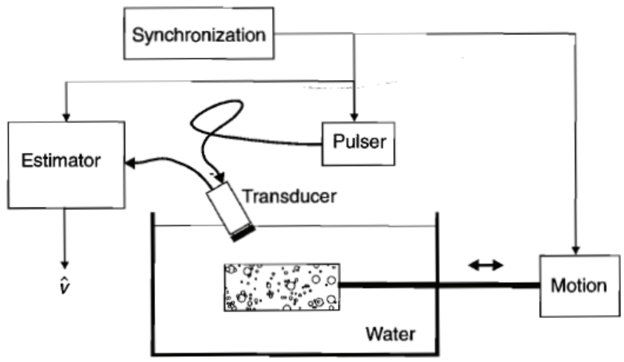


Fig. 4.4. Basic setup to illustrate Doppler effect and time shift effects.

**J.A.Jensen: Estimation of blood velocities using Ultrasound**

NTNU
Norwegian University of Science and Technology



40

# Continuous wave Doppler
# Doppler shift or time shift?

Reflector moving
Constant speed

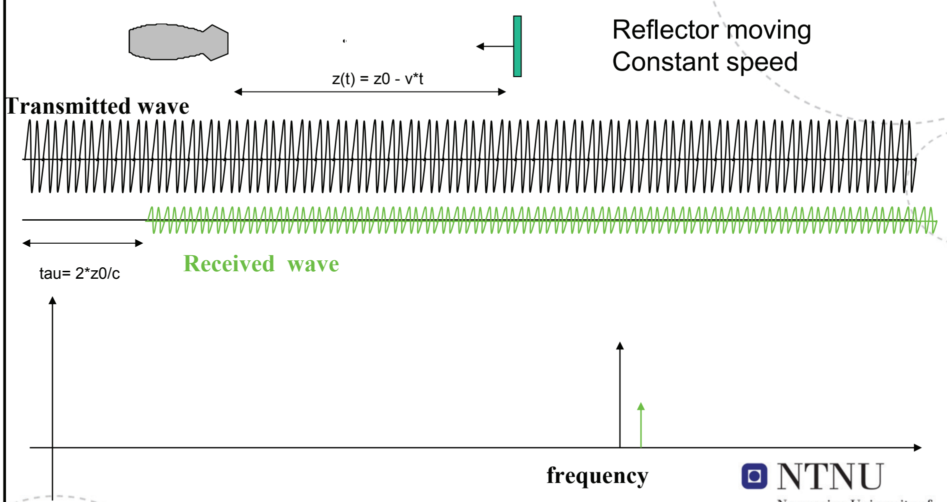


NTNU
Norwegian University of Science and Technology

# Pulsed wave Doppler
## Doppler shift or time shift?

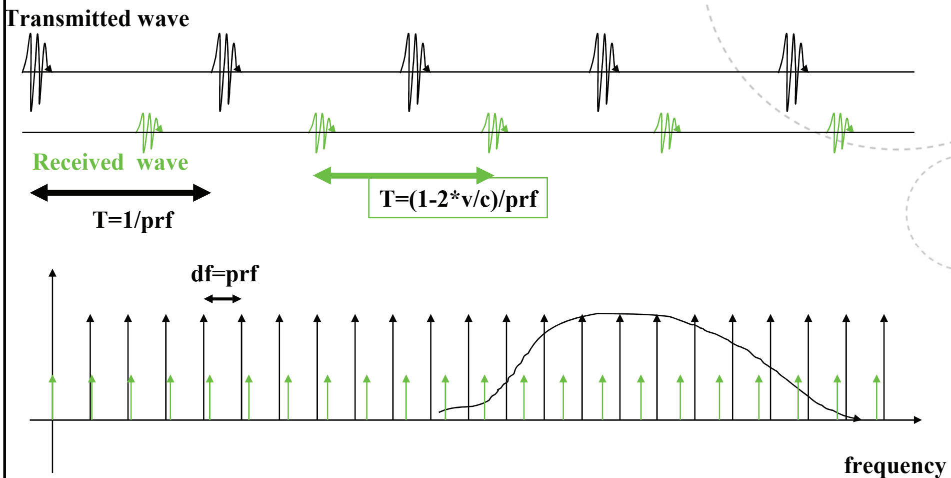








NTNU
Norwegian University of
Science and Technology

43

# Doppler Short Course '09

*Estimation and imaging blood flow velocity*

*Part II: Color Flow Imaging*

**2009 Ultrasonics Symposium, Rome, Italy**
Hans Torp and Lasse Løvstakken
Department of Circulation and Medical Imaging
Norwegian University of Science and Technology

NTNU
Norwegian University of Science and Technology



44

# Lecture outline

- General introduction to color flow imaging
  - Examples of clinical use, and a brief history lesson
- Data acquisition strategies
  - Acquiring the temporal sequence of samples
- Velocity estimation techniques
  - Estimation of Doppler signal parameters
- Clutter filtering
  - Attenuation of interfering signal from stationary tissue
- Display strategies in CFI

NTNU
Norwegian University of Science and Technology

45

# General introduction to CFI

NTNU
Norwegian University of Science and Technology



46

# Color flow imaging

- Displays a *color coded map* of the *axial* blood velocity in a 2-D or 3-D region of interest
- Used in a wide range of diagnostic contexts in today's hospitals

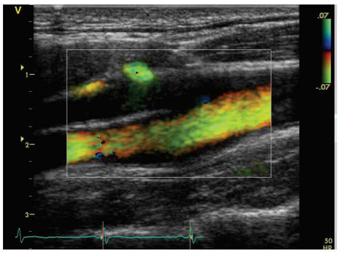

2-D CFI of a carotid bifurcation

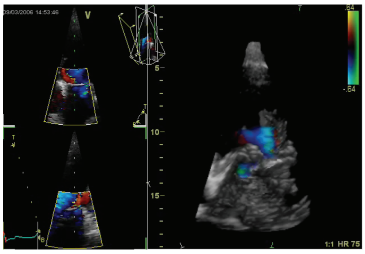

3-D CFI of a mitral regurgitation jet

NTNU
Norwegian University of Science and Technology

47

# Clinical examples

Mitral valve regurgitation jet

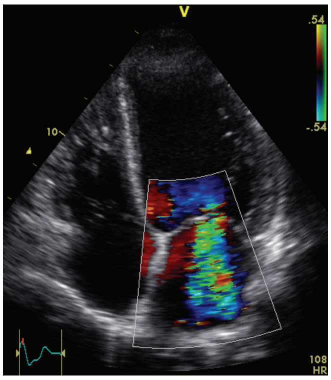

Atrial septum defect shunt flow

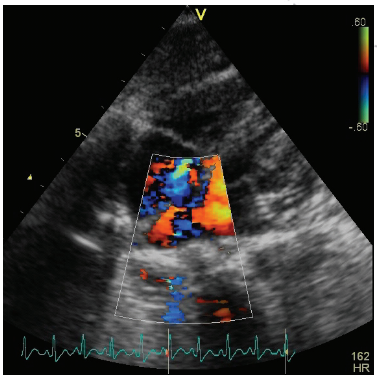



48

# More clinical examples

Carotid artery stenosis

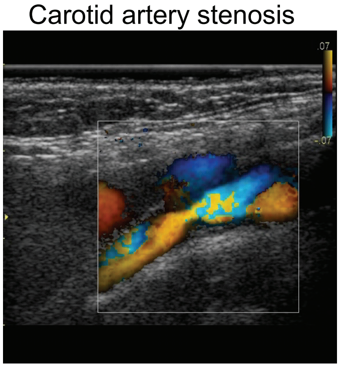

Thyroid nodule vascularization

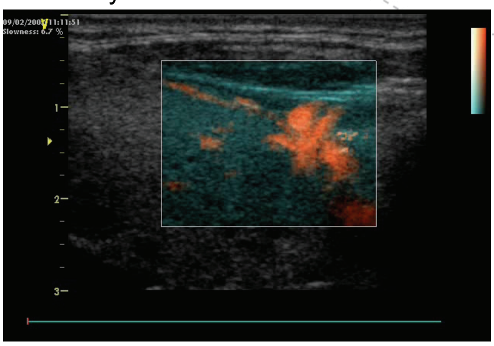

49

# A brief history lesson

- Technology and research progressed from single-range gate to multi-range gated Doppler, and further to 2-D Doppler imaging

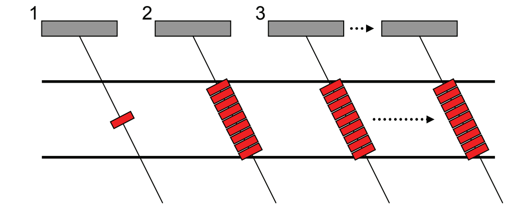


Single-range gate ➝ Multi-range gate ➝ 2-D Doppler

1

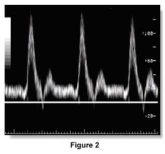


2

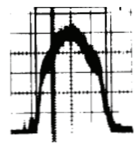

3

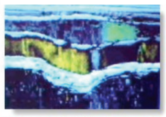

2-D color flow image of the carotid and jugular vein (top) from the Brandestini group in 1975

**Image source:** J. Woo, A short History of the development of Ultrasound in Obstetrics and Gynecology, *http://www.ob-ultrasound.net/history.html*

NTNU
Norwegian University of Science and Technology



50

# A brief history lesson

- Real-time CFI was first commercially available in the mid-eighties
  - Aloka (1985, Japan), Toshiba (1985, Japan), Quantum (1986, US), Vingmed (1986, Norway)

Aloka SSD-880CW

Quantum QAD-1

Vingmed CFM-700

**Source:** J. Woo, A short History of the development of Ultrasound in Obstetrics and Gynecology, *http://www.ob-ultrasound.net/history.html*

NTNU
Norwegian University of Science and Technology

51

# A brief history lesson

- However, real-time processing and display of color-Doppler images in weather RADAR was available ten years earlier (!)

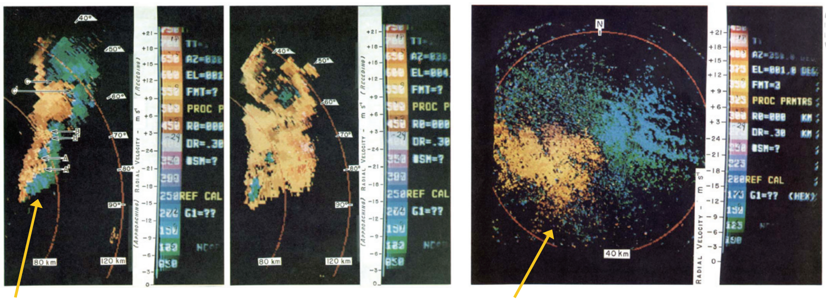

Storm signs

Insect signs

**Source:** G. R. Gray et al, Real-time color-Doppler RADAR display, *Bulletin of the American Meteorological Society*, vol. 56(6), 1975

NTNU
Norwegian University of Science and Technology



52

# CFI acquisition and processing

NTNU
Norwegian University of Science and Technology

53

# CFI processing chain

## Processing chain of conventional CFI

**Data acquisition** → **Clutter filtering** → **Parameter estimation** → **Display**

- CFI data acquisition
  – Scanning operation and pulse sequence
- Clutter filtering (wall filtering)
  – Attenuating interfering signal from stationary tissue
- Doppler parameter estimation
  – Estimation of Doppler power, mean-frequency, and bandwidth
- Display
  – Color encoding of Doppler parameters

NTNU
Norwegian University of Science and Technology



54

# Data acquisition in CFI

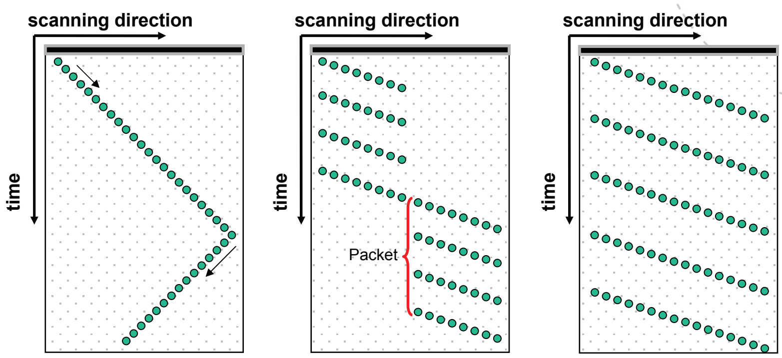


**Mechanical scanning**
+ No settling time for clutter filter
- Low frame rate

**Electronic packet scanning**
- Settling time for clutter filter
+ Flexible PRF without loss in frame rate

**Electronic continuous scanning**
+ No settling time for clutter filter
- High frame rate, but low PRF

NTNU
Norwegian University of Science and Technology

55

# Interleaved packet acquisition

**No interleaving**

Beam sequence ↓

| Beam position | | | | | |
|---|---|---|---|---|---|
| 1 | 5 | 9 | 13 | 17 | 21 |
| 2 | 6 | 10 | 14 | 18 | 22 |
| 3 | 7 | 11 | 15 | 19 | 23 |
| 4 | 8 | 12 | 16 | 20 | 24 |

Packet size = 4

$PRF_{max} = PRF_{user}$

**3 x beam interleaving**

| Beam position | | | | | |
|---|---|---|---|---|---|
| 1 | 2 | 3 | 13 | 14 | 15 |
| 4 | 5 | 6 | 16 | 17 | 18 |
| 7 | 8 | 9 | 19 | 20 | 21 |
| 10 | 11 | 12 | 22 | 23 | 24 |

Packet size = 4

$PRF_{max} = 3*PRF_{user}$

- Overall frame rate increased by the interleave factor
- Maximum PRF limited by image depth, multiple reflections, hardware
- Especially important when imaging low-velocity flow, i.e. with a low user chosen PRF such as peripheral vascular imaging

**Reference:** R. H. Chesarek, *Ultrasound imaging system for relatively low-velocity blood flow at relatively high frame rates.* USA, Patent no. 4888694, Quantum Medical System, Inc., 1989.

NTNU
Norwegian University of Science and Technology



56

# Packet / ensemble size in CFI

- Increasing the packet size in CFI will:
  - \+ Lead to more efficient clutter filtering
  - \+ Lower the variance of the Doppler parameters
  - – Reduce the overall frame rate dramatically
  - – May lead to visible artificial lags of the flow field in the image from one side of the image to the other
- How many samples are necessary?
  - – Application dependent, typically 8-16 samples
  - – Cardiac imaging (deep, high dynamics): packet size = 8-10
  - – Vascular imaging (shallow, lower dynamics): packet size = 10-16
  - – Abdominal imaging (deep, lower dynamics): packet size = 10-12

NTNU
Norwegian University of Science and Technology

www.ntnu.no H. Torp and L. Lovstakken - Doppler short course '09 - Part I:

# Signal-to-noise considerations

*Signal-to-noise is one of the most crucial design criteria in Doppler acquisition*

- Similar as for PW-Doppler: total SNR ~ 1/B, spectral SNR ~ $1/B^2$
- The received signal from blood is proportional to the length of the transmitted pulse (incoherent sum of burstlets)
  - Increase the number of pulse cycles
  - Decrease the pulse center frequency
- The optimal receive filter is approximatively given by a rectangular filter with length equal to the emitted pulse
  - Boxcar integrator over the pulse length
- Optimize TGC to achieve a constant noise floor throughout depth

**Reference:** K. Kristoffersen, *Optimal receiver filtering in pulsed Doppler ultrasound blood velocity measurements*, IEEE Trans. Ultrason., Ferroelec., and Freq. Contr., vol. 33(1), pp. 51-58, Jan. 1986





# CFI velocity estimation

59

# Doppler signal model

- The Doppler spectrum may consists of three components, clutter *c*, blood *b,* and thermal noise *n*

$$\mathbf{x} = \mathbf{c} + \mathbf{n} + \mathbf{b} \qquad \mathbf{x} = [x(1),\ldots,x(N)]^T$$

- Typical clutter/signal level: 20 – 80 dB
- Signal from blood is characterized by a complex Gaussian process

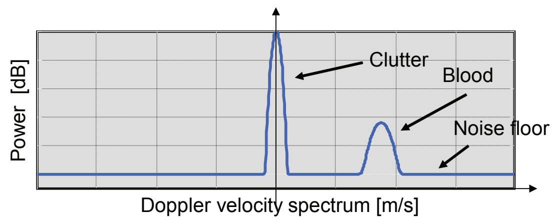


NTNU
Norwegian University of Science and Technology



60

# Doppler parameter estimation

Doppler parameter estimation in CFI has focused on the first three moments of the Doppler spectrum, which equals the mean power, mean frequency, and bandwidth (rms):

$$P = \int_{-\infty}^{\infty} G(\omega)d\omega \qquad \bar{\omega} = \frac{\int_{-\infty}^{\infty} \omega \cdot G(\omega)d\omega}{\int_{-\infty}^{\infty} G(\omega)d\omega} \qquad B_{rms}^2 = \frac{\int_{-\infty}^{\infty} (\omega - \bar{\omega})^2 \cdot G(\omega)d\omega}{\int_{-\infty}^{\infty} G(\omega)d\omega}$$

**However**: estimating the Doppler power spectrum and integrating is not a practical solution.

Time (phase) domain approaches has several qualities
- Less computationally expensive
- Robust in low signal-to-noise ratios
- Velocity range covering the full Nyquist spectrum width

NTNU
Norwegian University of Science and Technology

61

# Time domain formulation

The **Wiener-Khinchin** formula relates the autocorrelation function and the power spectral density function:

$$R(\tau) = \frac{1}{2\pi}\int_{-\infty}^{\infty} G(\omega)e^{j\omega\tau}d\omega$$

Derivatives with respect to tau gives:

$$\dot{R}(\tau) = \frac{j}{2\pi}\int_{-\infty}^{\infty} \underbrace{\omega G(\omega)e^{j\omega\tau}d\omega} \qquad \ddot{R}(\tau) = \frac{-1}{2\pi}\int_{-\infty}^{\infty} \underbrace{\omega^2 G(\omega)e^{j\omega\tau}d\omega}$$

Yields time-domain expressions for power, mean frequency, and bandwidth (rms):

$$P = R(0) \qquad \bar{\omega} = -j\frac{\dot{R}(0)}{R(0)} \qquad B^2 = \left[\frac{\dot{R}(0)}{R(0)}\right]^2 - \frac{\ddot{R}(0)}{R(0)}$$

NTNU
Norwegian University of Science and Technology



62

# The autocorrelation method

**However**: Accurate estimates of the derivatives of the autocorrelation function can be difficult to achieve. Therefore an alternative formulation is used:

Correlation function in polar form: $R(\tau) = A(\tau)\exp[j\phi(\tau)]$

Yields the following mean frequency and bandwidth estimate:

$$\bar{\omega} = -j\frac{\dot{R}(0)}{R(0)} = \dot{\phi}(0) \qquad \bar{\omega} \cong \frac{\phi(T_{PRF}) - \phi(0)}{T_{PRF}} = \boxed{\frac{1}{T_{PRF}}\arg[R(T_{PRF})]}$$

$$B^2 = -\frac{\ddot{A}(0)}{A(0)} \approx \frac{2}{T_{PRF}^2}\left[1 - \frac{A(T_{PRF})}{A(0)}\right] = \boxed{\frac{2}{T_{PRF}^2}\left[1 - \frac{|R(T_{PRF})|}{R(0)}\right]}$$

**In other words:** The power, mean frequency and bandwidth of the Doppler spectrum can be found using magnitude and phase estimates of the correlation function at lags 0 and 1 ($T_{PRF}$)

**Reference:** C. Kasai, *Real-Time Two-Dimensional Blood Flow Imaging Using an Autocorrelation Technique*, IEEE Transactions on Sonics and Ultrasonics, vol. 32 pp. 458-464, 1985

NTNU
Norwegian University of Science and Technology

63

# Autocorrelation method properties

- The ACM mean frequency estimate is unbiased for symmetric spectra, and approximatively so for narrow-band spectra

Alternative formulation: $R(\tau) = e^{j\bar{\omega}_d \tau} \int_{-\pi}^{\pi} G(\omega) e^{j(\omega - \bar{\omega}_d)\tau} d\omega$

The argument of R is equal to the (power-weighted) mean Doppler frequency $w_d$ if the imaginary part of the right side integral is zero:

$$\varepsilon = \int_{-\pi}^{\pi} G(\omega) \sin\left[(\omega - \bar{\omega}_d)\tau\right] d\omega = 0$$

This odd sine-weighting implies that only symmetric spectra will fulfill this criterion. However, approximatively so also for practical Doppler spectra

Since white noise has a symmetric spectrum, this implies that the autocorrelation estimator is unbiased in presence of white noise

NTNU
Norwegian University of Science and Technology

**Reference:** R. J. Doviak RJ and D. S. Zrnic, *Doppler RADAR and weather observations*. San Diego, Academic press, Inc., 1993.



64

# Autocorrelation method properties

- The mean frequency estimate is unbiased in the full Nyquist interval (for symmetric spectra)
  - Odd sine-weighting is centered at mean Doppler frequency

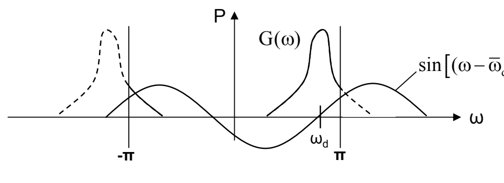


*Initial mean frequency estimators proposed for use in multi-range Doppler and CFI suffered from drop-outs when the velocity of blood was approaching the Nyquist limit.*

NTNU
Norwegian University of Science and Technology

**Reference:** R. J. Doviak RJ and D. S. Zrnic, *Doppler RADAR and weather observations*. San Diego, Academic press, Inc., 1993.

www.ntnu.no
H. Torp and L. Lovstakken - Doppler short course '09 - Part I:

65

# Autocorrelation estimator properties

- The variance of the autocorrelation estimator
  *Estimate correlation function by averaging over packet*
  - The variance of the power estimate *decreases* with increasing bandwidth

$$\mathrm{var}(\hat{P}) = \frac{1}{N}\sum_{k=-N}^{N}\left(1-\frac{|k|}{N}\right)\left|R(k)^2\right| \approx \frac{P^2}{BN}$$

P = signal power, B = signal bandwidth, N = ensemble (packet) size

  - The variance of the mean frequency estimate *increases* with increasing bandwidth

$$\mathrm{var}(\overline{\omega}_d) \sim \frac{B}{N}$$

*The variance of the autocorrelation estimates significantly improves by averaging the correlation estimates*

NTNU
Norwegian University of Science and Technology



66

# Autocorrelation estimator properties

- Robust in low signal-to-noise environments
  - Superior to FFT-based method below ~15 dB, similar above ~15dB
- Computationally inexpensive
  - Ideally, in a noise free environment only two complex samples are needed to estimate the mean frequency
  - In practice more samples are needed to 1) attenuate clutter, and 2) reduce the variance of the correlation estimates

NTNU
Norwegian University of Science and Technology

# Cross-correlation method

- The velocity is proportional to the RF time shift between successive pulses

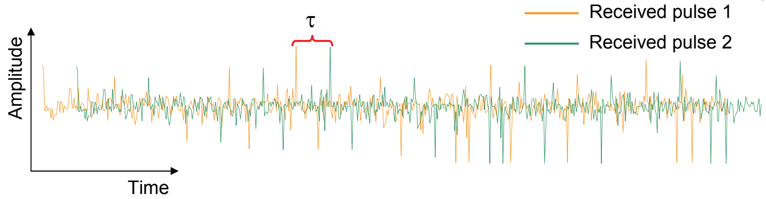


$$\tau = \frac{2\Delta z}{c} = \frac{2v\cos(\theta)T_{PRI}}{c} \qquad \hat{R}_{12}(m, m_0) = \frac{1}{N_S}\sum_{k=0}^{N_S-1} r_1(m_0 + k) r_2(m_0 + k + m)$$

$$\hat{\tau}_{max} = \arg\max \hat{R}_{12}(m) / F_s \qquad \hat{v}_z = \frac{c}{2}\frac{\hat{\tau}_{max}}{T_{PRI}}$$

**Reference:** O. Bonnefous and P. Pesque, *Time domain formulation of pulse-Doppler ultrasound and blood velocity estimation by cross correlation*, Ultrasonic imaging vol. 8, pp. 73-85, 1986.

NTNU
Norwegian University of Science and Technology





# Properties of the cross-correlation method

- No aliasing under ideal circumstances
  - Signal decorrelation and lateral movement will limit this however
- Best performance for wide-band pulses
  - Higher resolution / lower penetration
- Axial sampling determines jitter error
  - Interpolation needed to find the true correlation maximum
- Time shift does not directly transfer to *mean-velocity*
- Computationally expensive compared to autocorrelation method

NTNU
Norwegian University of Science and Technology

# Auto correlation vs. Cross correlation method

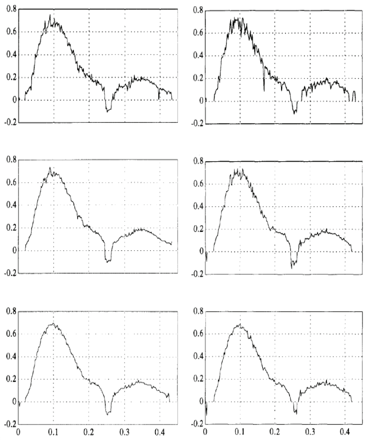

Autocorr.
No averaging

Auto corr.
1.6us averaging

Cross corr.
1.6us averaging

Narrow band

Wide band

**Example:**
*In vivo* Comparison of autocorrelation and cross-correlation for data from the human subclavian artery

*The two methods are approximatively equal for narrow-band pulses and with radial averaging*

***Reference:*** *Torp & al: Ultrasonic Symp. 93*

NTNU
Norwegian University of Science and Technology





# Clutter filtering

NTNU
Norwegian University of Science and Technology

71

# Clutter filtering

- Clutter is signal from surrounding tissue due to beam side lobes and reverberations
  - Can have 60-80 dB higher signal power than blood
- Blood typically has a higher velocity than tissue, i.e. higher Doppler shifts
  - The two components can thus be separated by high-pass filtering the Doppler signal

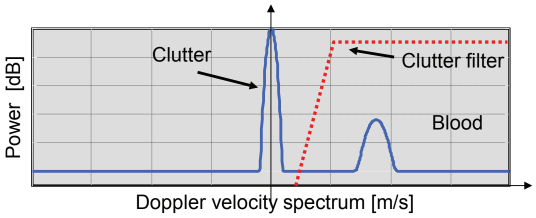




72

# General clutter filter design

- Clutter filters should have a *high stop-band attenuation* (60-80 dB) to sufficiently attenuate clutter
- Clutter filters should have a *short transition region* to avoid removing signal from blood

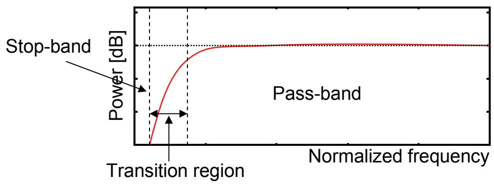


- Several filter types have been used:
  - Finite impulse response (FIR) filters, Infinite impulse response (IIR) filters, and polynomial regression filters

73

# Finite impulse response (FIR) filters

**Example**: Filter order M=5, packet size N=10

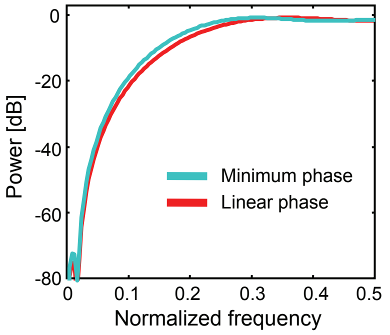


- The filter output *y* is the weighted sum of *M* past inputs *x*:

$$y(n) = \sum_{k=0}^{M-1} h(k)x(n-k)$$

- Discard the first *M* output samples, where *M* is equal to the filter order
- Improved amplitude response when nonlinear phase is allowed

NTNU
Norwegian University of Science and Technology

**Source:** S. Bjærum et al, Clutter Filter Design for Ultrasound Color Flow Imaging, *IEEE Trans. Ultrason., Ferroelec., and Freq. Contr.*, vol. 49(2), pp. 204-216, Feb. 2002



74

# Linear or non-linear phase response

- Conventional color flow imaging algorithms are based on the correlation function of the filtered signal

$$R_y(m) = \frac{1}{2\pi}\int_{-\pi}^{\pi} S_x(\omega)|H(\omega)|^2 e^{jm\omega}d\omega$$

(A linear transformation of the correlation function)

Doppler spectrum Filter frequency response

- This means that it is safe to disregard the phase response when designing FIR clutter filters
- Without phase response constraints, an improved filter frequency response can be achieved for a given filter order
  - Minimum-phase response filters have the smallest time delay and most asymmetric impulse response

NTNU
Norwegian University of Science and Technology

**Reference:** S. Bjærum et al, Clutter Filter Design for Ultrasound Color Flow Imaging, *IEEE Trans. Ultrason., Ferroelec., and Freq. Contr.*, vol. 49(2), pp. 204-216, Feb. 2002

75

# Infinite impulse response (IIR) filters

**Example:** Chebyshev order M=4, packet size N=10

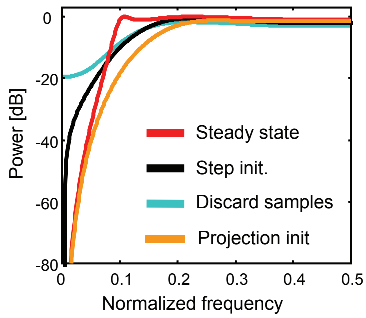


- The filter output *y* is the weighted sum of past and current inputs *x* and past outputs *y*:

$$y(n) = -\sum_{k=1}^{M} a(k)y(n-k) + \sum_{k=0}^{M} b(k)x(n-k)$$

- Variations: Butterworth, Chebyshev, Elliptic
- *Filter initialization* is critical to dampen the transient response (recursive filter)
- Chebyshev filter with projection initialization preferred for color flow imaging applications


1. E. S. Chornoboy, Initialization for improved IIR filter response, IEEE Trans. Signal processing, vol. 40(3), March 1992
2. S. Bjærum et al, Clutter Filter Design for Ultrasound Color Flow Imaging, IEEE Trans. Ultrason., Ferroelec., and Freq. Contr., vol. 49(2), pp. 204-216, Feb. 2002


NTNU
Norwegian University of Science and Technology



76

# Regression filters

- The clutter *c* is estimated as a least squares fitting of the signal *x* to a set of basis functions $\mathbf{b}_k$
  - A projection operation from the complex vector space $\boldsymbol{C}^N$ to the clutter subspace $\boldsymbol{B}^K$ spanned by basis functions $\mathbf{b}_k$

$$c = \mathrm{proj}_B(x) = \sum_{k=1}^{K} \langle x, b_k \rangle b_k$$

- The clutter component is subtracted from the signal, which can formulated as a matrix operation

$$y = \underbrace{\left(I - \sum_{k=0}^{M-1} b_k b_k^{*T}\right)}_{\text{Projection matrix}} x = Ax$$

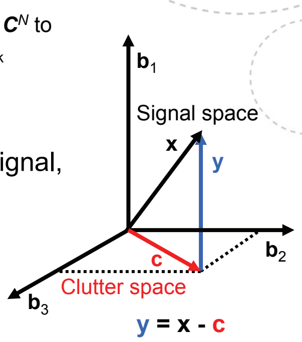



1. A. P. G. Hoeks et al. An efficient algorithm to remove low frequency signals in digital Doppler systems. Ultrasound Imaging, vol. 13, pp. 135-144, 1991
2. H. Torp, Clutter rejection filtering in Color Flow Imaging: a theoretical approach, IEEE Trans. Ultrason., Ferroelec., and Freq. Contr., vol. 44(2), pp. 417-424, Feb. 1997


NTNU
Norwegian University of Science and Technology

77

# Choice of basis functions

- The choice of clutter basis functions has a large impact on performance

**Fourier basis:**

$$b_k = \frac{1}{\sqrt{N}} e^{jkn/N}, \quad n = 0, \ldots, N-1$$

Orthonormal and equally distributed in frequency

**Analogy:**

1. Discrete Fourier transform
2. Set low frequency coefficients to zero
3. Inverse Fourier transform

**Example:** N=10, clutter dim. K=3

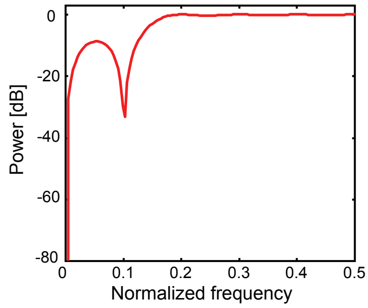


NTNU
Norwegian University of Science and Technology



78

# Legendre polynomial basis

- A set of orthonormal polynomials: $\int_{-1}^{1} P_m(x) P_n(x) dx = \delta_{mn}$

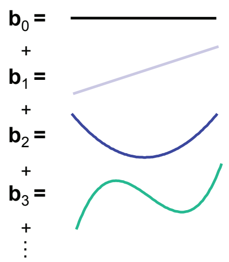


$$y = \left( I - \sum_{k=0}^{M-1} b_k b_k^{*T} \right) x = Ax$$

**Example:** N=10, clutter dim. K=1-4

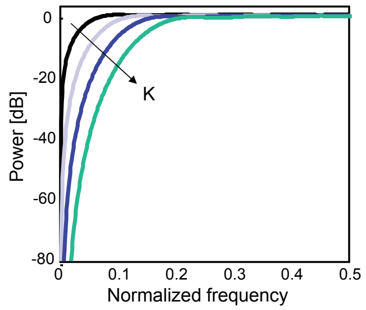


The Legendre polynomials can be generated through a Gram-Schmidt orthonormalization procedure on the polynomials $x^k$, k=0,…,K

NTNU
Norwegian University of Science and Technology

79

# Linear clutter filter formulation

**Why should clutter filters be linear?**

- No intermodulation between clutter and blood signal
- Preservation of signal power from blood
- Optimum detection (Neuman-Pearson test) includes a linear filter

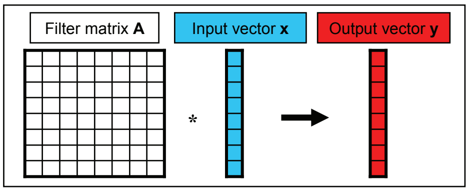


*Any linear filter can be performed by a matrix multiplication of the N-dimensional signal vector x*

**y = Ax**

*This form includes all IIR filters with linear initialization, FIR filters, and regression filters*

NTNU
Norwegian University of Science and Technology



80

# FIR filter matrix structure

$$A = \begin{bmatrix} b_1 & b_2 & b_3 & b_4 & b_5 & b_6 & 0 & . & . & 0 \\ 0 & b_1 & b_2 & b_3 & b_4 & b_5 & b_6 & & & . \\ . & & b_1 & b_2 & b_3 & b_4 & b_5 & b_6 & & . \\ . & & & b_1 & b_2 & b_3 & b_4 & b_5 & b_6 & 0 \\ 0 & . & . & 0 & b_1 & b_2 & b_3 & b_4 & b_5 & b_6 \end{bmatrix}$$

| | |
|---|---|
| FIR filter order | M=5 |
| Packet size | N=10 |
| Output samples | N-M= 5 |

Increasing filter order

- \+ Improved clutter rejection
- \- Increased estimator variance

NTNU
Norwegian University of Science and Technology

# Frequency response of linear filters

- The frequency response of linear filters is defined as the filter output for a single frequency complex sinusoid input

$$H_0(\omega) = \frac{1}{N}\left\|Ae_\omega\right\|^2, \quad -\pi < \omega < \pi \qquad e_\omega = [1\, e^{j\omega} \ldots e^{j(N-1)\omega}]^T$$

**Note:** The output of the filter is not in general a single frequency signal. This is only the case for FIR filters.

**Note:** Frequency response is only well-defined for complex signals

**Reference:** H. Torp, *Clutter rejection filtering in Color Flow Imaging: a theoretical approach*, IEEE Trans. Ultrason., Ferroelec., and Freq. Contr., vol. 44(2), pp. 417-424, Feb. 1997

NTNU
Norwegian University of Science and Technology





# CFI display algorithms

NTNU
Norwegian University of Science and Technology

# Color mapping types

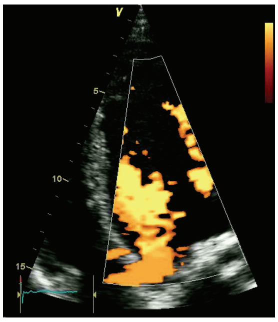

**Power Doppler** (Angio)
Brightness ~ signal power

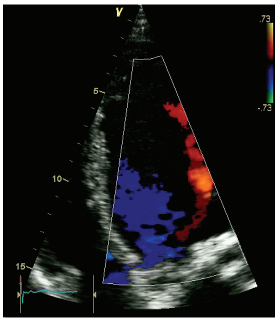

**Color flow**
Brightness ~ signal power
Hue ~ Velocity

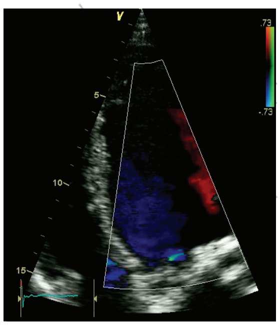

**Color flow ”Variance map”**
Hue & Brightness ~ Velocity
Green ~ signal bandwidth

**Image example :** Aortic regurgitation





# Tissue / flow arbitration

- B-mode and CFI image acquired separately due to the resolution / penetration requirements / comprimises in CFI and B-mode
- The two images are typically combined through a hard decision of whether to display a B-mode or color pixel → *Arbitration*
- Post-processing is also needed in order to reduce the amount of flashing artifacts due to insufficient clutter attenuation

  This decision is typically based on:
  - Mean frequency and power before and after filtering
  - High power / low frequency (below filter cut-off) => tissue

# Arbitration examples

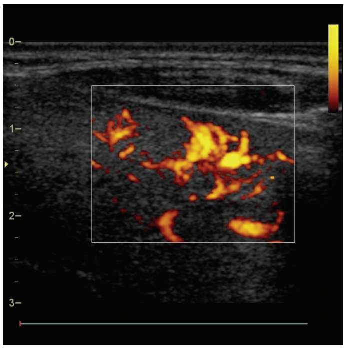


**Power-Doppler:** Hard arbitration

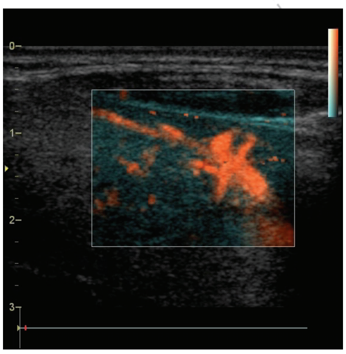


**Power-Doppler:** Soft arbitration

**Example:** Thyroid nodule vascularization

NTNU
Norwegian University of Science and Technology





# Topics not covered here

- Advanced axial velocity estimators
  - Techniques utilizing 2-D signal information
- Synthetic transmit aperture flow imaging
  - Lots of interesting aspects investigated
- Coded excitation in color flow imaging
  - When is it feasible?
- B-Flow imaging
  - Simultaneous acquisition of B-mode and flow images
  - Coded excitation to retain both resolution and penetration

- And more…

NTNU
Norwegian University of Science and Technology

# Doppler Short Course ‘09

*Estimation and imaging blood flow velocity*

*Part III: Advanced topics, trade-offs and limitations*

**2009 Ultrasonics Symposium, Rome, Italy**
Hans Torp, Lasse Løvstakken
Department of Circulation and Medical Imaging
Norwegian University of Science and Technology

NTNU
Norwegian University of Science and Technology





# Limitations of current Doppler / CFI techniques

NTNU
Norwegian University of Science and Technology

89

# Limitations of CFI

- Conventional methods suffer from several fundamental limitations that restrict its use in clinical practise

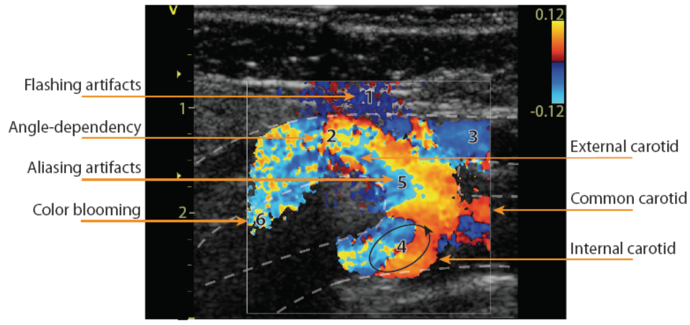




90

# Data acquisition limitations

- Sufficient signal-to-noise ration vs. spatial resolution
  - The spatial resolution typically needs to be lowered compared to B-mode to achieve a sufficient SNR
  - This leads to *color blooming artifacts* in CFI where the color image smears into the B-mode image
- Frame rate vs. estimator quality vs. lateral sampling
  - The packet size and number of image lines is reduced in order to achieve a sufficient frame rate for following the flow dynamics
  - In real-time 3-D CFI, frame rate is a particular challenge

NTNU
Norwegian University of Science and Technology

91

# Clutter filtering limitations

- Clutter is often not properly attenuated during the whole cardiac cycle
  - This leads to *flashing artifacts* where tissue regions are falsely colored as blood
- Clutter filtering performance vs. packet size
  - Due to frame rate requirements, the number of samples available for clutter filtering is limited → long filter transition regions
- Clutter effect on velocity estimates
  - Signal varying bias towards zero if not properly attenuated
  - The clutter filter may also remove substantial blood signal if the angle is near transverse

NTNU
Norwegian University of Science and Technology



92

# Velocity estimator limitations

- Only the axial velocity component is measured
  - Measured velocities depend on the angle between the ultrasound beam and vessel of interest →*angle-dependency artifacts*
  - For transverse flow, the mean Doppler shift is centered around zero, and a substantial part is removed by the clutter filter
- Aliasing artifacts
  - A limited velocity range can be measured before *aliasing* occurs, determined by the PRF
  - Using a higher PRF increases the maximum limit, but sensitivity to low velocities is then reduced (in practice due to clutter filter)
- Bias / variance
  - The bias and variance can in practice be quite high, and varies in space and time → the use of CFI has mainly been of qualitative nature

NTNU
Norwegian University of Science and Technology

# Patient safety in Doppler imaging

NTNU
Norwegian University of Science and Technology





# Patient safety in Doppler imaging

- Potential hazardous heating and mechanical effects restrict the allowed acoustic output of ultrasonic imaging equipment
- Acoustic output is restricted by one of the following:
  - Mechanical index (MI), a measure of mechanical effects
  - Spatial peak temporal average intensity (Ispta), total output power, or thermal index (TI)
  - Transducer surface temperature
- Heating effects are averaged for combinations of modes (duplex / triplex modes). Mechanical effects are determined by the modality with the highest value.

**The outcome:** The sensitivity / penetration in Doppler modes may be severly punished from these restrictions

NTNU
Norwegian University of Science and Technology

# Mechanical effects

- Mechanical effects are related to cavitation, i.e. the formation and collapse of gas bubbles

***Mechanical index:*** $MI = \frac{p_{r.3}(z_{sp})}{\sqrt{f_{awf}}}$ → Derated peak rarefactional pressure → Acoustic working frequency

*Focal gain:* $G_{foc} = \frac{D_a D_e}{R_{foc}\lambda} = \frac{D_e}{F_{\#}\lambda} = \frac{D_e \cdot f_0}{F_{\#} \cdot c}$ (Coinciding az. an el. Foci)

→ MI is measured at the axial point of maximum *derated* temporal averaged intensity ($I_{ta}$)

→ **MI is effectively proportional to applied voltage, sqrt(f0), and inverse proportional to the F-number**

NTNU
Norwegian University of Science and Technology





# Tissue heating

- Heating occur in the tissue due to absorption, at a rate much lower (~seconds) than the ultrasound frame rate
- **Spatial-peak temporal average intensity (Ispta):**

$$I_{spta} = \max_z \left[ PRR \cdot \int_0^{T_{PRR}} p_z^2(t) / \rho c \, dt \right]$$

- Proportional to the transmitted pulse energy
- Proportional to the squared focal gain, $G_{foc}$
- For scanned modes, the intensity contributions for overlapping beams are added

NTNU
Norwegian University of Science and Technology

97

# Transducer surface heating

- **FDA regulations:** The transducer surface may not exeed *43 deg. held towards the skin*, or *50 deg. towards air*
- For current transducer technology, surface heating is almost always higher than at the geometric focus[1]
  → *It is typically the most limiting factor with regards to voltage / PRF / apertures*
- The temperature rise for duplex and triplex modes (B-mode+CFI+PW-Doppler) is an average for a common time constant (frame rate / PRF)

**Reference:** [1] M. Curley, *Soft Tissue Temperature Rise Caused by Scanned, Diagnostic Ultrasound*, IEEE Trans., Ultrason., Ferroelect., and Freq. Contr., vol. 40(1), Jan 1993

NTNU
Norwegian University of Science and Technology



98

# Transducer surface heating

- Empirical model of surface temperature:

$$\Delta T(x) = \sum_{n=1}^{N_e} W_n \times \Delta T_n(x)$$

$\Delta T_n(x)$: Temperature increase for element *n* at position *x* along the surface

$W_n$: The number of times element *n* is fired

$$\Delta T_n(x) \sim \frac{PRF \cdot V^2 \cdot \bar{\beta}(f_0, B_0)}{2\alpha} \cdot g(x \mid x_n, D_{ap}, \alpha)$$

**Legend:** PRF = pulse repitition frequency, V = voltage over element, α = measured thermal conductivity / efficiency parameter, β = measured pulse parameter, $D_{ap}$=aperture width, $x_n$=element *x* position

**Temperature rise is proportional to PRF, $V^2$, g(aperture), pulse length, …**

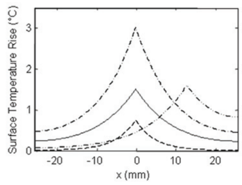


Temperature rise $\Delta T_n(x)$ for different transducer elements

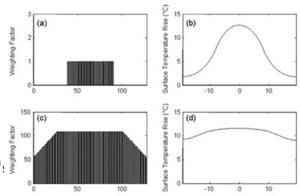


Different weighting factors, Wn.
*Top:* PW-Doppler, *bottom:* scanned

**Reference:** W.-S. Ohm et al, *Prediction of Surface Temperature Rise of Ultrasonic Diagnostic Array Transducers*, IEEE Trans., Ultrason., Ferroelect., and Freq. Contr., vol. 55(1), Jan 2008

# PW-Doppler acoustics

- For a nonscanning situation, the maximum Ispta is close to the focal region
- The longer pulses typically used in PW-Doppler significantly increases heating effects
- For duplex operation (B-mode + PW-Doppler), surface temperature increase is mostly dominating
- For triplex operation (B-mode+CFI+PW-Doppler), Ispta or surface temperature will dominate

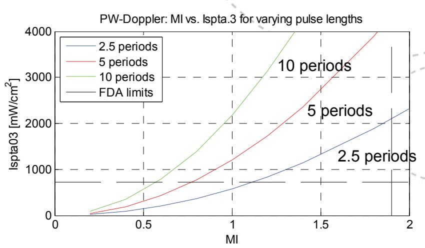


**Setup:** Linear array, f0 = 5MHz, FNtx = 2.5, txFocus 4 cm, *PRF = 8kHz*

**Outcome: PW-Doppler is typically Ispta limited**, exceptions include very low PRFs, low frequencies, and narrow focusing

NTNU
Norwegian University of Science and Technology





# Color Flow Imaging acoustics

- For a scanning situation, the maximum Ispta is close to the surface
- Similar characteristics for phased-array (cardiac) probes as for linear array (vascular) probes
- Duplex operation adds heating effects from B-mode
- Generally surface temperature limited
- MI limited only for short pulses, low frequencies and PRFs, narrow focusing

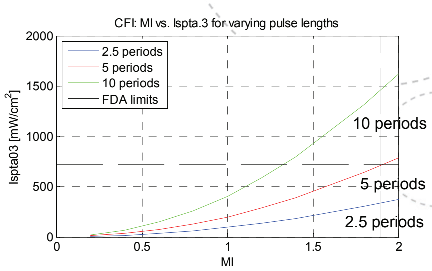


**Setup:** Linear array, f0 = 5MHz, FNtx = 2.5, txFocus 4 cm, *PRF = 4kHz,* 2 cm ROI width, 50 beams. **NB: B-mode values not added**

**CFI is typically transducer surface temperature limited.** Exceptions include very low PRFs, low frequencies, and narrow focusing

NTNU
Norwegian University of Science and Technology

# Surface temperature comparison

- An example of surface temperature prediction for PW vs. CFI for the same aperture / tx-focus
- CFI generates a higher surface temperature then PW-Doppler due to:
  - Aperture overlap during scanning, i.e. individual elements are excited more often,
  - The imaging PRF is often higher in CFI than for PW-Doppler

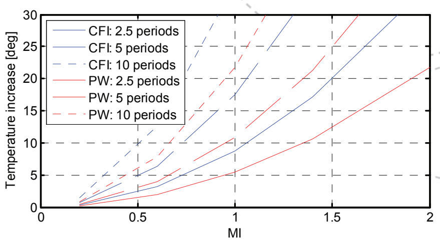


**Common setup:** Linear array, f0 = 5MHz, FNtx = 2.5, txFocus 4 cm

**CFI:** PRF_img = 16kHz, PRF=4kHz, Np=12, 2 cm ROI width, 50 beams.

**PW:** PRF_PW = 8kHz, Np=64

**NB: B-mode values not added**





# Patient safety summary

- Transducer surface heating is currently the main limitation in CFI and B-mode+PW-Doppler, while $I_{spta}$ is the main limitation in CW- and PW-Doppler (without B-mode)
  - MI limitations might occur for low PRFs, short pulses, and narrow focusing
- For an equal PRF, the temporally average transmitted energy is distributed over a larger spatial region for scanned modes than for PW-Doppler:
  - Lowering overall tissue heating effects for scanned modes
  - Bringing the maximum temperature close to the transducer for scanned modes
  - Especially the case for 3-D imaging
- These rules of thumb apply to both linear array (vascular) as well as phased array (cardiac) imaging

NTNU
Norwegian University of Science and Technology

103

# Coded excitation in Doppler

- Using *non-linear phase-modulation* can increase the pulse length without reducing the bandwidth, and may therfore be used to increase the amount of transmitted energy
- *Deconvolution filtering* on receive restores the phase to retain axial resolution
- The theoretical improvement in SNR is equal to the *time-bandwidth product* of the transmitted waveform, *TB.*
  - I.e., for a given bandwidth, doubling the pulse length by coding may theoretically double the SNR

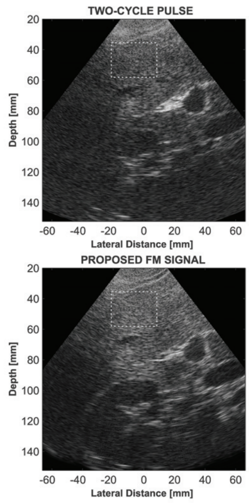


**Reference:** T. Misaridis and J. A. Jensen, *Use of Modulated Excitation Signals in Medical Ultrasound. Part I: Basic Concepts and Expected Benefits*, IEEE Trans., Ultrason., Ferroelect., and Freq. Contr., vol. 52(2), Feb 2005



104

# When is coded excitation applicable in Doppler modes?

- Codes are in general applicable only when MI-limited
- As previously indicated, heating effects are typically prominent and will severely limit the advantage of codes in Doppler modes
- Disregarding surface heating, a potential might however exist for codes in CFI
  - More efficient transducer materials
  - Active cooling
  - Unfocused imaging (MI ~ $G_{foc}$, $I_{spta}$ ~ $G_{foc}^2$, → $G_{foc}$= 1)

NTNU
Norwegian University of Science and Technology

10
5

# Advanced axial velocity estimators

NTNU
Norwegian University of Science and Technology



10
6

# 2-D Doppler signal representation

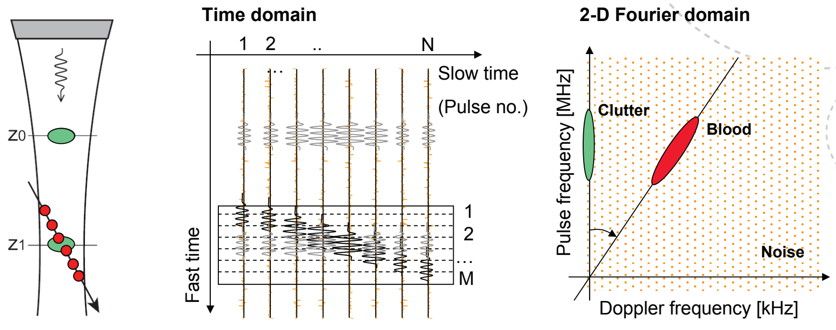


*This 2-D representation contains the total signal information available for processing*

NTNU
Norwegian University of Science and Technology

10
7

# 2-D spectrum example

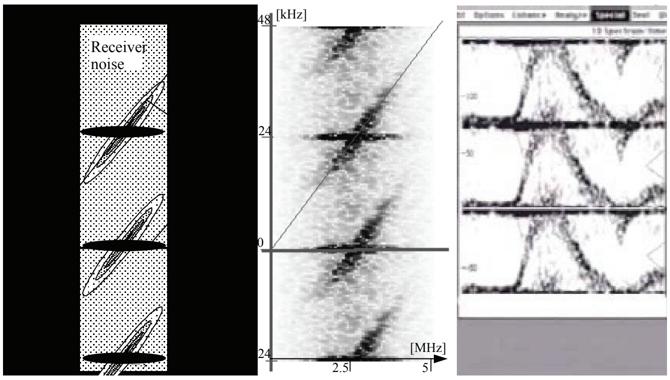


Theoretical 2D spectrum

Estimated 2D spectrum

Estimated 1D spectrum



10
8

# Velocity matched spectrum algorithm for PW-Doppler

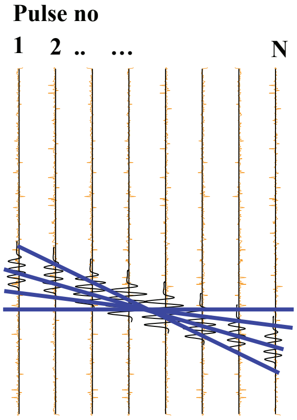


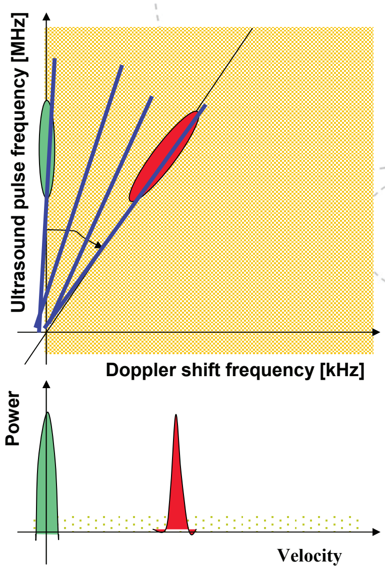

10
9

# Blood velocity spectrum
## Subclavian Artery

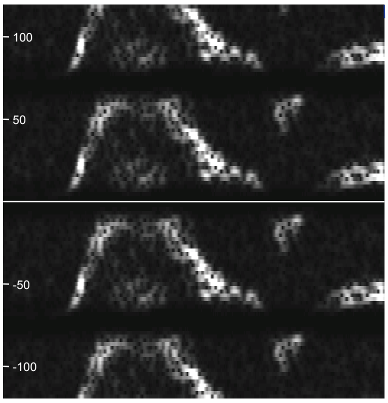


Conventional spectrum

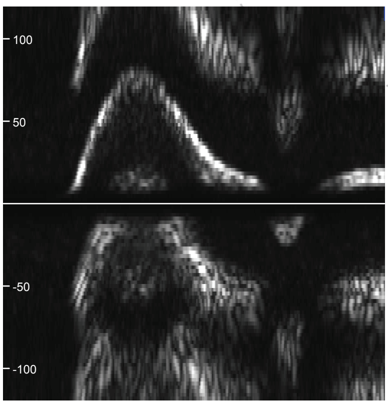


Velocity matched spectrum



11
0

# Advanced velocity estimation in Color Flow Imaging

- The autocorrelation approach is a *a* **narrow-band technique** that only utilizes a portion of the signal information available
- Several **wide-band velocity estimators** have been proposed, some examples:
  - Cross-correlation technique
  - 2-D spectral processing techniques
  - Wide-band maximum likelihood estimator
- These methods may outperform the ACM with regards to accuracy and aliasing limit

NTNU
Norwegian University of Science and Technology

111

# Disadvantages of wide-band processing

- Wide-band, i.e. short pulses are needed, which may lead to SNR problems
- Decorrelation limits the practical velocity range that may be tracked beyond the Nyquist range
- Substantially increased computational load

NTNU
Norwegian University of Science and Technology



112

# Adaptive clutter filtering

NTNU
Norwegian University of Science and Technology

11
3

# Adaptive clutter filtering in CFI

- An adaptive filter has a data dependent response
- Adapting the clutter filter to clutter characteristics may:
  - Reduce flashing artifacts by more effecively attenuating clutter
  - Remove less blood signal throughout the cardiac cycle
- Especially relevant in:
  - Low-flow environments
  - Excessive tissue movement environments

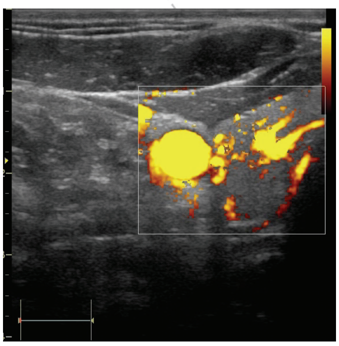

**Example:** Flashing artifacts when imaging an healthy carotid artery and thyroid (low PRF)

NTNU
Norwegian University of Science and Technology



11
4

# The downmixing approach

**Algorithm:**

- Estimate the main tissue Doppler frequency, $\omega_t$
- Downmix the signal with $\omega_t$ prior to conventional clutter filtering

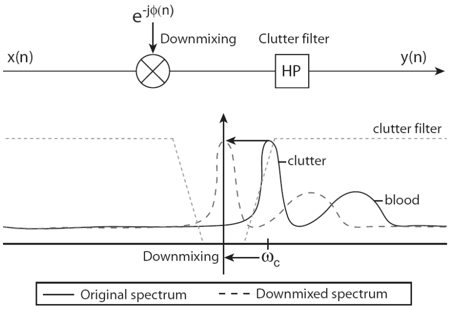


**Reference:** L. Thomas and A. Hall, An improved wall filter for flow imaging of low velocity flow, Proceedings of the IEEE Ultrasonics Symposium, 1994

NTNU
Norwegian University of Science and Technology

115

# The downmixing approach

- The clutter Doppler frequency is obtained using the autocorrelation approach on spatially averaged data
- Downmixing can be done based on the estimated *mean frequency* of clutter, or the *instantaneous frequency* of clutter

**Mean frequency:**

$$\phi_{mf}(n) = \hat{\omega}_C n = \angle\left[\sum_{k=1}^{N_P-2} \hat{R}(k,1)\right] n$$


**Instantaneous frequency:**

$$\phi_{if}(n) = \begin{cases} 0 & n = 0 \\ \left[\sum_{k=1}^{n} \angle\hat{R}(k,1)\right] & n = 1, \ldots, N-2 \end{cases}$$

NTNU
Norwegian University of Science and Technology

**Reference:** S. Bjærum et al, Clutter Filter Design for Ultrasound Color Flow Imaging, *IEEE Trans. Ultrason., Ferroelec., and Freq. Contr.*, vol. 49(2), pp. 204-216, Feb. 2002



116

# The downmixing approach

- Downmixing filters are in general quite robust, however:
  - Stationary tissue signal can be shifted *into* the pass band of the clutter filter
  - Instantaneous frequency downmixing may lead to *artifacts* in the shifted Doppler spectrum
- Downmixing with the *instantaneous* clutter Doppler frequency provides superior clutter suppression
- A *combined approach* is possible where:
  - Detection and arbitration of blood is done with instantaneous frequency downmixing and filtering
  - Velocity estimation is performed after mean frequency mixing and filtering

NTNU
Norwegian University of Science and Technology

117

# The eigen-based concept

**Background**

- The clutter contribution to signal variation is different then from blood

  **Typically:** The clutter component is more dominant (higher energy) and infers more low-frequency variation than blood

**Filter principle**

- Principal component analysis (PCA) / the Karhunen Loeve expansion (KLE) separates the main sources of variation
- By selecting the modes of variation based on *a priori* knowledge of clutter, a signal basis can be found and used to attenuate clutter

NTNU
Norwegian University of Science and Technology



118

# Eigen-based algorithm

1. Estimate correlation matrix
   Average in a spatial region
2. Signal decomposition
   Estimate eigenvectors and eigenvalues, i.e. the orthogonal signal basis functions in PCA
3. Identify clutter eigen-components
   Based on a priori assumptions
   For instance the most dominant in energy
4. Form filter matrix and filter
   Regression / projection filtering approach

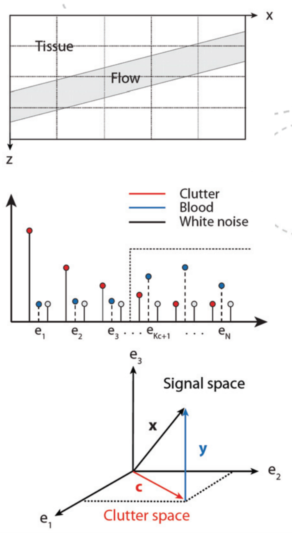

11
9

# The eigen-based formulas

- Signal model consists of up to *three independent components*, clutter *c*, noise *n*, and optionally blood *b*

$$x = c + n + b \qquad R_x = R_c + R_n + R_b$$

- The signal correlation matrix is estimated by **spatial averaging**

$$\hat{R}_x = \frac{1}{M}\sum_{m=1}^{M} x_m x_m^{*T}$$

- The clutter is represented by the orthonormal basis given by **selected eigenvectors** of the signal correlation matrix

$$x = \sum_{k=1}^{N_D} \gamma_k e_k, \quad E\{\gamma_k \gamma_l^*\} = \begin{cases} \lambda_k, & k = l \\ 0, & k \neq l \end{cases}$$

- Filtering is performed as for regression filters through **projection**

$$P = I - \sum_{k=1}^{K_c} e_k e_k^{*T}$$

NTNU
Norwegian University of Science and Technology



12
0

# An eigen-spectrum example

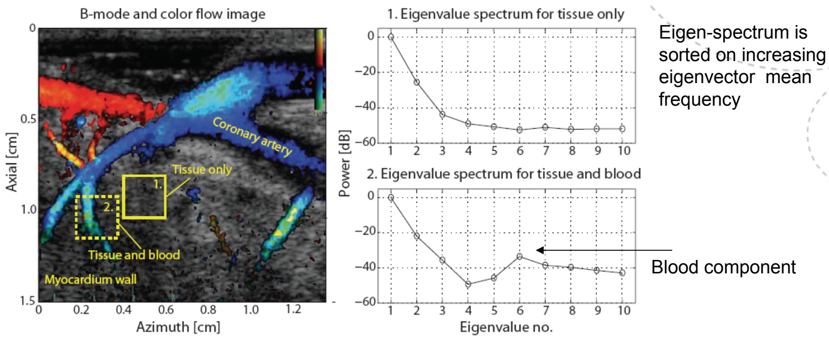


**Eigen-spectrum** for 1) tissue+noise, and 2) tissue+blood+noise

**Image example:** Epicardial imaging of porcine myocardium at 14 MHz

NTNU
Norwegian University of Science and Technology

# Eigen-based filter examples

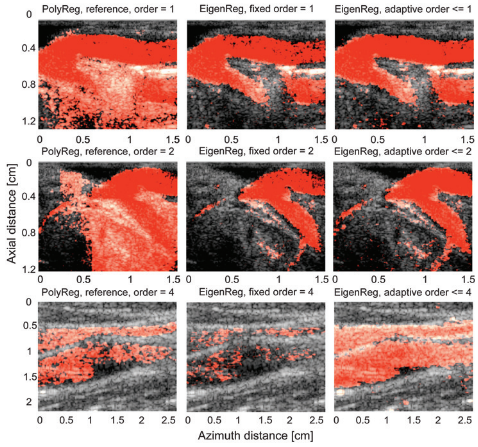


**Clutter filtering examples:**
1-2: Coronary artery bypass
3: Carotid artery

All example frames are from the systole with maximum tissue movement. 40 dB dynamic range for tissue, 6 dB dynamic range for flow

**Observations:**
1. Eigen-based method provides an improved suppression of clutter

2. If too many eigenvectors are included in clutter basis, then blood signal is lost

**Reference:** L. Løvstakken et al, Real-time adaptive clutter rejection filtering in color flow imaging using power method iterations, *IEEE Trans. Ultrason., Ferroelec., and Freq. Contr.*, vol. 53(9), pp. 1597-1608, Sept. 2006

NTNU
Norwegian University of Science and Technology





# Downmixning vs. eigen-approach

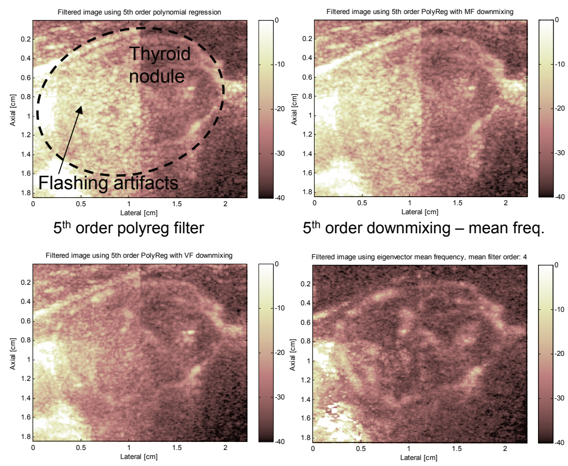


5th order polyreg filter
5th order downmixing – mean freq.
5th order downmixing - instantaneous
Eigen-filter – adaptive order

**Example:**
Thyroid gland tumor nodule, raw power-Doppler image, PRF = 250 Hz (extreme)

**General observations:**
The eigen-approach achieves superior clutter suppression for lower order filters

The eigen-approach is dependent on an adaptive selection of filter order

Instantaneous downmixing performs quite well in general

The downmixing filters in general seem more robust

NTNU
Norwegian University of Science and Technology

# Comparison movies

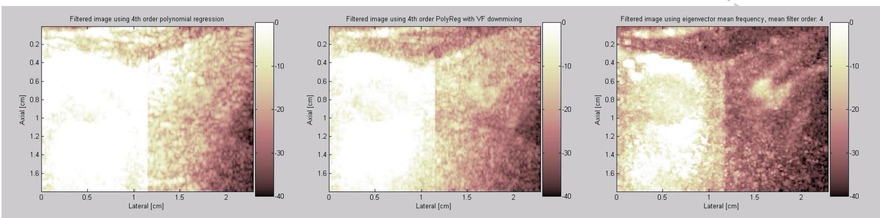


4$^{th}$ order polyreg filter — 4$^{th}$ order downmixing - instantaneous — Eigen-filter – adaptive order

**Example:**

Thyroid gland tumor nodule, raw power-Doppler image, PRF = 250 Hz (very low)





# Summary – adaptive clutter filtering

- Eigen-based filtering can provide superior clutter suppression for low filter orders in regions with excessive tissue motion, however:
  - The filter order must be chosen adaptively for different regions of the image for robust performance
  - Spatial averaging of the correlation matrix estimate smoothes the resulting flow images
- Downmixing filtering can provide an improved suppression of clutter in general, however:
  - Stationary signal may be shifted into the pass band
  - Artifacts may appear in the Doppler spectrum when using a varying (instantaneous) downmixing frequency

125

# Doppler Short Course '09

*Estimation and imaging of blood flow velocity*

*Part IV: Future directions*

**2009 Ultrasonics Symposium, Rome, Italy**

Hans Torp and Lasse Løvstakken
Department of Circulation and Medical Imaging
Norwegian University of Science and Technology



126

# Lecture outline

- 2-D vector velocity imaging of blood
  - Vector-Doppler, speckle tracking, echo-PIV
- High frame rate Color Flow Imaging
  - Parallel beamforming, plane-wave imaging, synthetic aperture flow imaging, multi-transmit CFI
- Real-time 3-D ultrasound applications
  - 3-D color flow imaging, high-PRF 3-D imaging of mitral valve leakage

12
7

# 2-D velocity vector imaging

NTNU
Norwegian University of
Science and Technology



12
8

# 2-D blood vector velocity mapping

- Vector-Doppler techniques
  - Combine Doppler shift from spatially separated transmit / receive apertures
- Speckle imaging / tracking techniques
  - Visualization of speckle pattern movement
  - Tracking of speckle pattern movement
- Transit-time broadening techniques
  - The bandwidth of the Doppler signal is related to the lateral velocity component
- Synthetic aperture techniques
  - Beamforming and cross-correlation along arbitrary lines. Choosing the direction of maximum correlation

NTNU
Norwegian University of
Science and Technology

# Vector-Doppler techniques

- Compound Doppler techniques
  - Combine Doppler shift from several physically / electronically separated transmit / receive apertures
- Lateral oscillation techniques
  - Common transmit aperture, spatially separated receive apertures created electronically using "non-uniform" apodization functions
  - Transverse oscillation method (TO) (Jensen 1998)
  - Spatial quadrature method (SQ) (Anderson 1998)

NTNU
Norwegian University of Science and Technology





# Compound Doppler method
## with common transmit beam

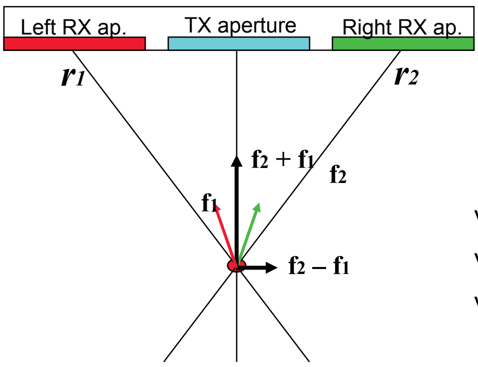


**f1** : Doppler shift left aperture

**f2** : Doppler shift right aperture

Velocity components:

Vx = (λ/2) (f2 - f1)

Vz = (λ/2) (f2 + f1)

US patent 93 Anne Hall, GE, Crossing beam Color flow imaging
Expanding aperture

NTNU
Norwegian University of Science and Technology

13
1

# Spatial quadrature technique

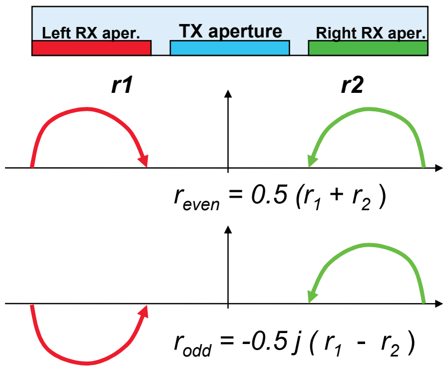


$$r_{even} = 0.5\,(r_1 + r_2)$$

$$r_{odd} = -0.5\,j\,(r_1 - r_2)$$

An *oscillation in the lateral field* is created using a non-uniform receive apodization function (left/right receive)

The left / right receive apertures are separated using quadrature relations

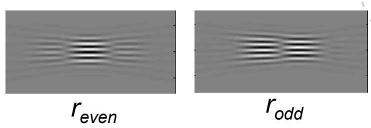


**Reconstruction:**

$$r_1 = r_{even} + j\,r_{odd}$$

$$r_2 = r_{even} - j\,r_{odd}$$


**Reference:** M. E. Anderson. *Multi-dimensional velocity estimation with ultrasound using spatial quadrature.* IEEE Trans., Ultrason., Ferroelect., and Freq. Contr., vol. 45(3), pp. 852-861, May 1998


NTNU
Norwegian University of Science and Technology



13
2

# Transverse oscillation technique

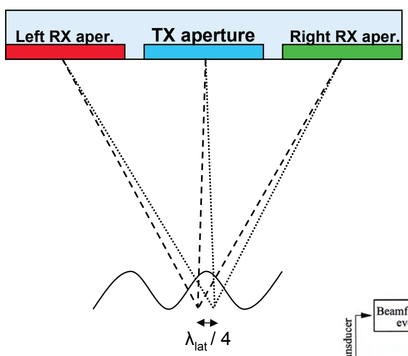


An *oscillation in the lateral field* is created using a non-uniform receive apodization function (left/right receive)

The left / right receive apertures are separated by *sampling* beams *one quarter lateral wavelength* apart

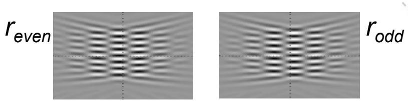


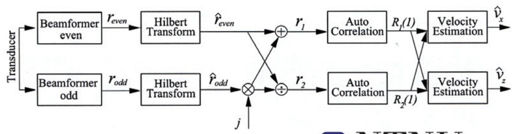



**References:**

J. A. Jensen and P. Munk. *A new method for estimation of velocity vectors.* IEEE Trans., Ultrason., Ferroelect., and Freq. Contr., vol. 45(3), pp. 837-851, May 1998

J. Udesen and J. A. Jensen. *Investigation of Transverse Oscillation Method.* IEEE Trans., Ultrason., Ferroelect., and Freq. Contr., vol. 53(5), pp. 959-971, May 2006


NTNU
Norwegian University of Science and Technology

13
3

# Compound Doppler vs TO comparison

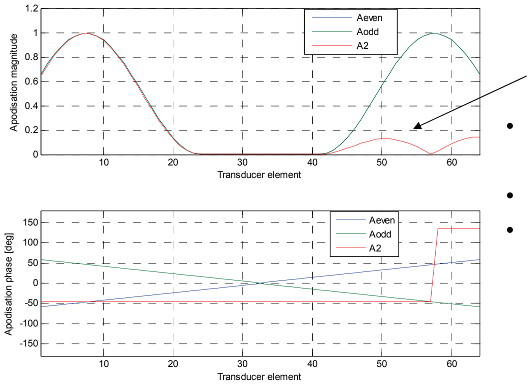


- SNR-ratio analysis:
  TO method - 0.11 dB
- Mirror spectral energy: 29 dB
- No significant velocity bias when using autocorrelation method

NTNU
Norwegian University of Science and Technology



13
4

# Summary of vector Doppler methods

- *Spatial quadrature* and *compound Doppler* are identical methods
- *Transverse oscillation* method is approximately equal to *compound Doppler* method for small apertures and narrowband pulses
- All three methods give approximatively equal performance for typical aperture / pulse bandwidths

NTNU
Norwegian University of Science and Technology

135

# Blood speckle imaging

- The speckle pattern from blood flow signal is isolated by high-pass filtering the Doppler signal
- The movement of this speckle pattern is correlated to the movement of blood

Tissue echo speckle pattern

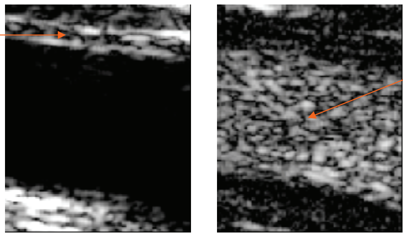

Blood flow echo speckle pattern

**Figure:** B-mode image of carotis artery and corresponding filtered image showing the blood flow speckle pattern utilized in BFI

NTNU
Norwegian University of Science and Technology



136

# Blood Flow Imaging

*Speckle movement visualization*

- Speckle pattern images of moving blood is captured at **a high frame rate**, and is played back in **slow motion**
- The movement of the blood flow speckle pattern can then be **visually tracked from image to image**

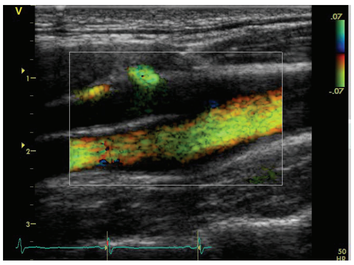

**Figure:** A visualization of the speckle pattern movement from blood in a carotid bifurcation

Speckle images are superimposed onto conventional Doppler images

**Reference:** L. Lovstakken *et al. Blood Flow Imaging - A New Real-Time, 2-D Flow Imaging Technique*. IEEE Trans., Ultrason., Ferroelect., and Freq. Contr., vol. 53(2), pp. 289-299, Feb 2006

NTNU
Norwegian University of Science and Technology

137

# BFI - signal processing

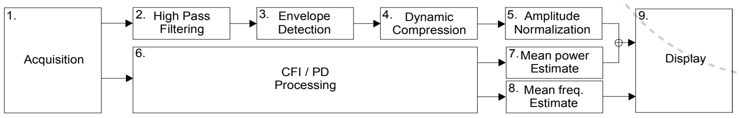


- High-pass filtering produce signal from blood
  - Time-invariant FIR filters preserve speckle pattern similarities
- B-mode processing produces speckle images
- Amplitude normalization
  - Reduce signal power discontinuities between frames
- Combine with CFI
  - Modulate the parametric color images with speckle pattern images
  - Interpolate color images in time to match the number of speckle images

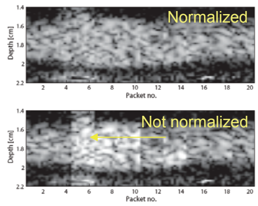


**Figure:** Normalization needed to reduce discontinuities between image frames

NTNU
Norwegian University of Science and Technology



138

# BFI example 1 – vascular imaging

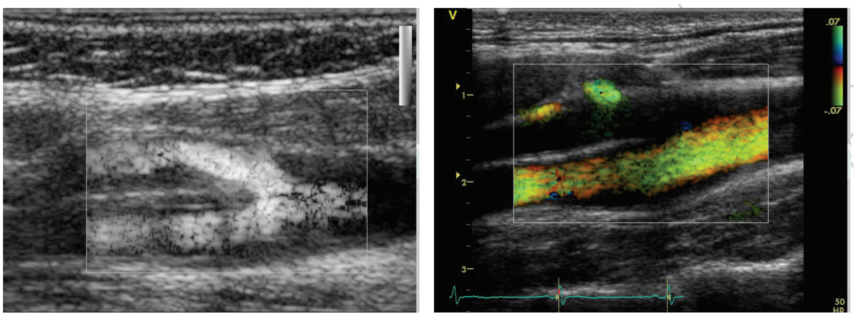

**Vascular imaging**

Imaging of a stenosed carotid bifurcation

Left: Power Doppler + speckle, right: CFI + speckle

NTNU
Norwegian University of Science and Technology

www.ntnu.no
H. Torp and L. Lovstakken - Doppler short course '09 - Part I:

# BFI example 2 – coronary bypass surgery

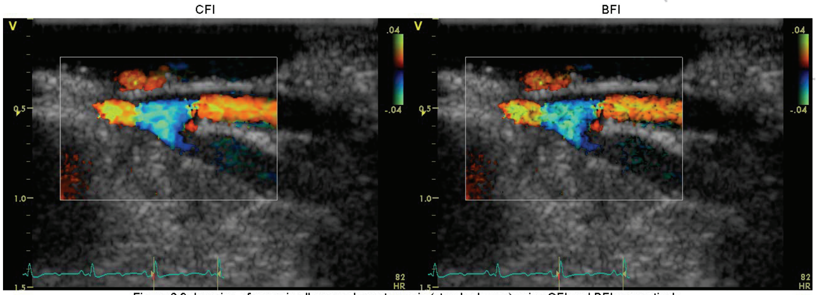


Figure 6.3: Imaging of a proximally snared anastomosis (standard case) using CFI and BFI respectively.
L. Løvstakken, K. S. Ibrahim, N. Vitale, S. T. Hendriksen, I. Kirkeby-Garstad, H. Torp, and R. Haaverstad,
"Blood Flow Imaging - A new 2-D ultrasound modality for enhanced intraoperative visualization of blood flow patterns in coronary anastomoses"

**Intraoperative imaging in cardiothoracic surgery**

Imaging of a proximally occluded (snared) LIMA-LAD bypass anstomosis, using CFI (left) and BFI (right)

NTNU
Norwegian University of Science and Technology





# Speckle tracking of blood

- Tracking speckle pattern between subsequent frames, speckle displacement is given by best match

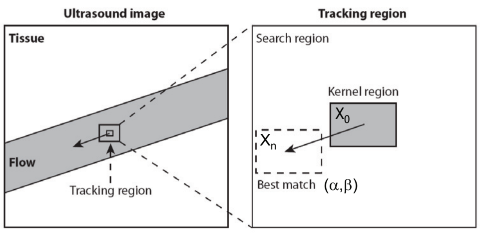


**Sum of Absolute Differences (SAD):**

Block matching algorithm

Real-time operation feasible (special purpose multimedia instructions)

Displacement given for minimal SAD:

$\varepsilon_{min} = (\alpha_m, \beta_m)$

$$\varepsilon(\alpha,\beta,n) = \sum_{i=1}^{l}\sum_{j=1}^{k}\left|X_0(i,j) - X_n(i+\alpha, j+\beta)\right| \qquad V_n = \frac{\sqrt{(\alpha_m \Delta x)^2 + (\beta_m \Delta z)^2}}{nT} \qquad \vartheta_n = \arctan\frac{\alpha_m \Delta x}{\beta_m \Delta z}$$

G. E. Trahey *et al. Angle Independent Ultrasonic Detection of Blood Flow.* IEEE Trans., Biomed. Eng., vol. 34(12), pp. 965-967, Dec 1987

L. N. Bohs *et al. Speckle tracking for multi-dimensional flow estimation.* Ultrasonics, vol. 38, pp. 369–375, 2000

NTNU
Norwegian University of Science and Technology

# Speckle tracking challenges

- Speckle decorrelation

  The speckle pattern decorrelates rapidly due to:
  a) Spatial and temporal velocity gradients
  b) Non-laminar flow
  c) Out-of-plane movements

- Clutter filtering
  - Doppler-based high-pass filtering removes blood signal for near-transversal flow
  - Reduces SNR, and influences the speckle appearence

NTNU
Norwegian University of Science and Technology





# Speckle tracking acquisition

A *very high frame* rate is needed due to the rapid decorrelation

- **Interleaved / parallel beam acquisition**
  - Speckle region frame rate equal to the user chosen PRF
  - Two-way resolution / penetration
  - Time lag across image as in conventional color flow imaging

- **Plane wave acquisition**
  - Single unfocused transmit beam, all receive channels available
  - Continuous acquisition, processing from frame to frame
  - High overall frame-rate (~100 Hz), no time lags across image
  - Reduced resolution and penetration → coded excitation

NTNU
Norwegian University of Science and Technology

14
3

# Plane wave emission

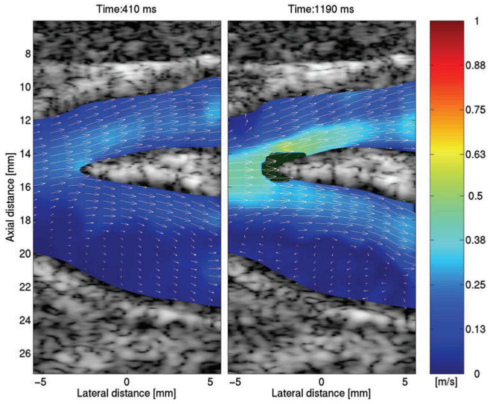


- Unfocused transmit beam
- Receive channel data available
- One speckle image for each transmit pulse
- 13 bit barker codes
- Resolution ~ 1x1 mm
- Frame-to-frame clutter filtering
- Frame rate 100 Hz

J. Udesen et al, "Fast Blood Vector Velocity Imaging: Simulations and Preliminary in vivo Results", Proceedings of IEEE Ultrasonics Symposium, New York 2007

NTNU
Norwegian University of Science and Technology



14
4

# Speckle tracking vs. vector-Doppler

- By simulating ultrasound signals from realistic flow fields obtained using computational fluid dynamics, experimental methods can be evaluated and compared statistically in a controlled manner

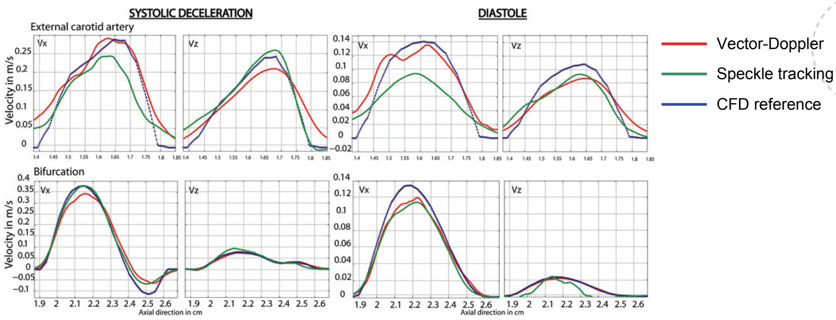


*A. Swillens et al., Ultrasonics Symposium 2008, Beijing, China*

NTNU
Norwegian University of Science and Technology

145

# Speckle tracking vs. crossed-beam vector Doppler

- Simulated data from a carotid artery bifurcation model (CFD)
- Comparison movie for a clutter filtered example at 2kHz PRF

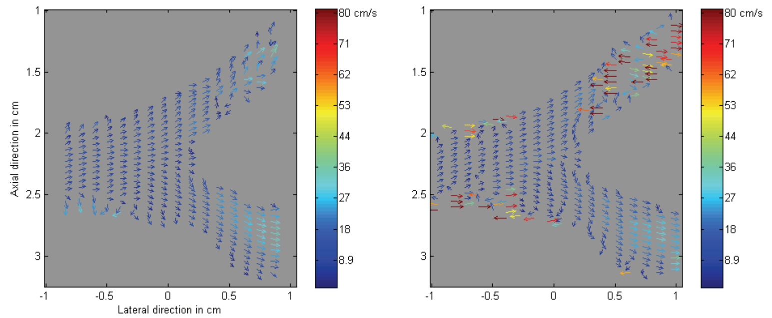


Speckle tracking — Crossed-beam vector Doppler

*A. Swillens et al. Oral presentation given at blood flow session Wednesday, 23. Aug.*



146

# Clutter filtering in 2-D velocity estimation

- Doppler-based clutter filtering will remove signal from blood as the beam-vessel angle approaches 90°
- Vector-Doppler
  - Signal drop-out for tx/rx aperture from one side
- Speckle tracking
  - Signal drop-out for near transversal flow
  - Remaining signal becomes band pass also laterally → lateral oscillations

***One of the main challenges in 2-D velocity estimation***

NTNU
Norwegian University of Science and Technology

147

# Clutter filtering effect on the speckle images

- Axial and lateral object movement is equal to a rotation of the system point spread function around the $k_z$-$\omega$ and $k_x$-$\omega$ axes in *k-space*
- Ideal clutter filter removes all signal below a threshold $\omega$-plane
- The remaining signal may become *band-pass* in both $k_z$ and $k_x$

**K-space representation:**

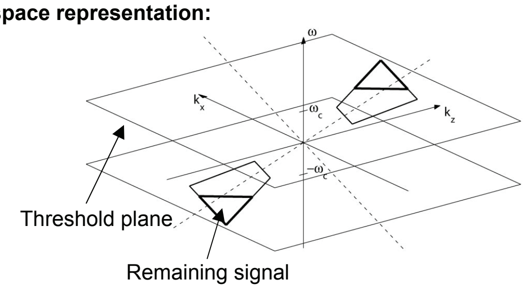


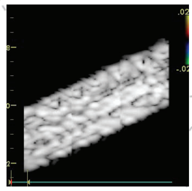

FIR filtered, ~60 deg

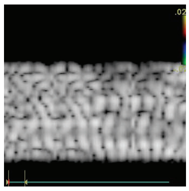

FIR filtered, ~90 deg



148

# Echo particle image velocimetry (Echo-PIV)

- Tracking the movement of small concentrations of injected contrast bubbles
- Avoids problems with clutter filtering and low SNR
- Can be used to estimate flow-derived parameters such as wall shear rate

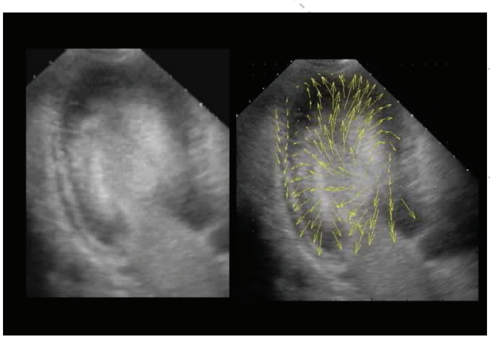

**Example:** Left ventricle flow patterns by Echo-PIV

**Reference:** G.-R. Hong et al. *Characterization and Quantification of Vortex Flow in the Human Left Ventricle by Contrast Echocardiography Using Vector Particle Image Velocimetry*, JACC: Cardiovascular Imaging, Volume 1, Issue 6, November 2008

149

# Summary – 2-D velocity estimation

- Compound vector-Doppler and lateral oscillation methods give basically the same performance

- Both vector-Doppler and speckle tracking are able to resolve the axial *and* lateral velocity component, however:
  a) Clutter filtering will cause signal drop-outs for both methods
  b) Vector-Doppler accuracy is dependent on the angle between tx and rx apertures, limiting the depth and width of the scan possible
  c) The receive apertures are limited in vector-Doppler (single array operation) leading to a reduction in signal-to-noise ratio
  d) Speckle tracking is dependent on a very high frame rate due to speckle decorrelation, especially for complex flow patterns
  e) Speckle tracking is dependent on spatial interpolation in order to achieve accurate displacement estimates



150

# High frame rate CFI

NTNU
Norwegian University of Science and Technology

15
1

# Increasing the frame rate in CFI

**Generate several receive lines per transmit**

- Parallel receive beamforming
- Plane-wave flow imaging
- Synthetic aperture flow imaging

**Multiple transmit pulses**

- Disjoint in frequency, filtering on receive to separate

**Decrease the ensemble size**

- More advanced clutter filtering is needed

NTNU
Norwegian University of Science and Technology

www.ntnu.no H. Torp and L. Lovstakken - Doppler short course '09 - Part I:

15
2

# Parallel receive beamforming

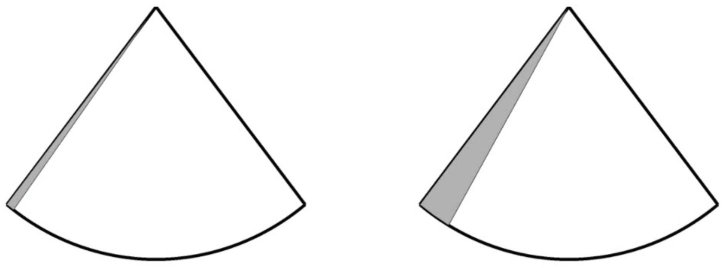

**Conventional image formation:**

An image is built line by line, one for each ultrasound transmission

**Parallell receive beamforming:**

*N* image lines are generated per ultrasound transmission
*Frame rate increased by N times*

www.ntnu.no Animations by S. A. Aase H. Torp and L. Lovstakken - Doppler short course '09 - Part I:

153

Find out more at the poster presentation by T. Hergum in the Beamforming session at this years conference

# Parallel receive beamforming

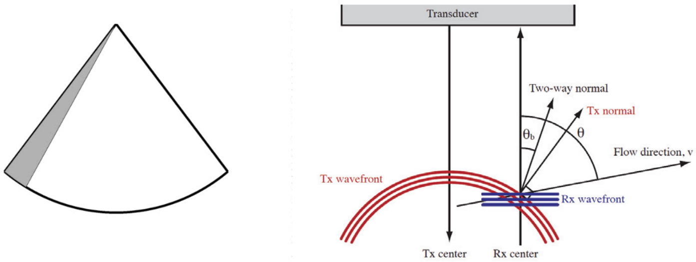


+ *N* image lines are generated per ultrasound transmission, i.e. **frame rate increases by *N***. Based on traditional focused beams on transmit.
- The **curvature of focused transmit beams** leads to a Doppler angle varying across the group of parallel receive beams
- For a large number of PRB the **transmit aperture becomes very small**

**Reference:** T. Hergum et al., *Reducing Color Flow Artifacts caused by Parallel Beamforming*, IEEE Trans. Ultrason., Ferrielect. And Freq. Contr. *submitted, 2009*



154

# Plane-wave imaging

- Plane-waves are **unfocused ultrasound beams**, **without curvature** over a limited depth
- One transmitted plane-wave can illuminate a large spatial region so that **a high number of parallel receive beams can be utilized**
- Due to the flat curvature, **image artifacts** normally associated with parallel receive beamforming for focused beams **are avoided**
- **Trade-off:** A significant loss in transmitted pressure compared to focused beams

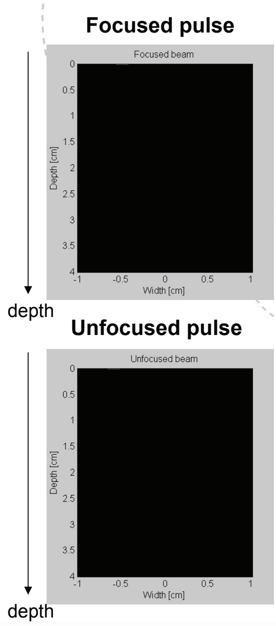

155

# What is the difference?

*An illustration of the frame rate difference for the same amount of image lines (fully sampled). Playback is at 20% of real-time.*

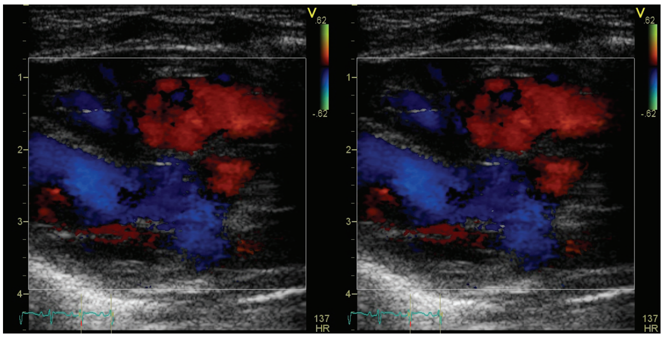

Equivalent to current high-end acquisition, **2x parallel beams**

Plane wave imaging, **16x parallel beams** (both B-mode and CFI)

**Image example:**

Neonate heart with an atrium-ventricular septum defect. Parasternal cross-section.

*More examples are shown at this years conference, Wednesday 23. Sept at the oral Blood Flow session*



156

# Synthetic aperture flow imaging

- One emission results in a complete image with low resolution and SNR
- By combining several low-resolution images a high-resolution image is produced

**Pros and cons**

+ Continuous acquisition
+ Flexible beamforming
- SNR issues
- Computational demands
- Motion artifacts due to inadequate compensation of movement for high-resolution images

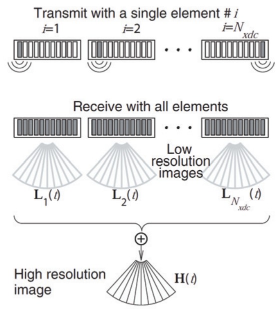


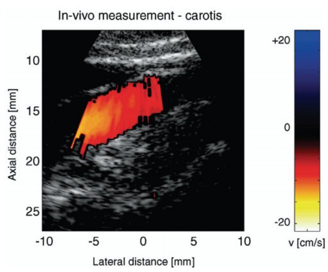


**Reference:** S. I. Nikolov and J. A. Jensen, *In-Vivo Synthetic Aperture Flow Imaging in Medical Ultrasound*, IEEE Trans. Ultrason., Ferrielect. And Freq. Contr. vol. 50, no. 7, July 2008

157

# Multiple transmit pulses

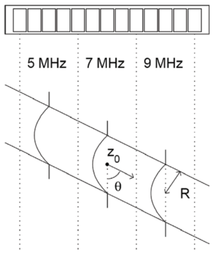


- Emit *N* wide-band transmit pulses simultaneously in different directions
- Filter signals from disjoint (narrow-band) frequency bands on receive

**Pros and cons**

\+ Increases the frame rate by *N*
\+ Conventional focused beams
\+ May be combined with parallel receive beamforming
\- Varying estimator quality for different frequency bands
\- Varying Nyquist velocity for each band
\- Varying SNR for each band

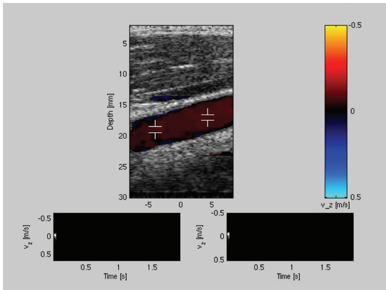


**Reference:** N. Odderhede et al, *Multi-Frequency Encoding for Fast Color Flow or Quadroplex Imaging*, IEEE Trans. Ultrason., Ferrielect. And Freq. Contr. vol. 55, no. 4, April 2008



158

# Real-time 3-D imaging

NTNU
Norwegian University of Science and Technology

159

# 3D color flow imaging with 2-D matrix array probe

From 1D Array…

64 – 128 array elements

to 2D Array…

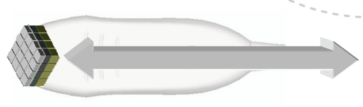

2000 – 3000 array elements

**Challenges:**
Long data acquisition time, stitching data from 7 heart cycles
Small element size → high electrical impedance → lower SNR

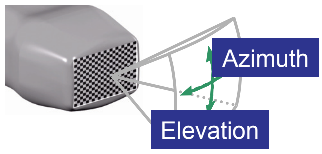


NTNU
Norwegian University of Science and Technology



160

# Real-time 3-D CFI example

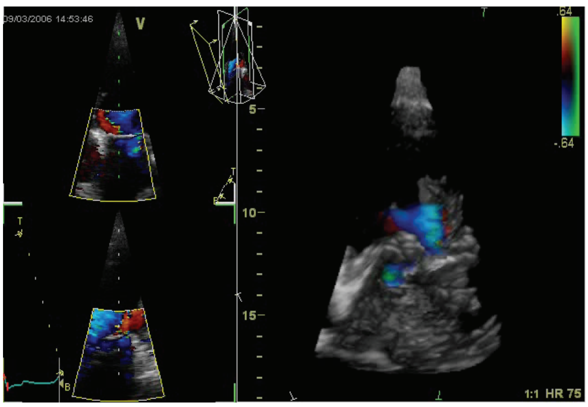


**Example:**

Mitral valve insufficiency

Real-time CFI without ECG triggering and volume stitching

**The main challenge is frame rate**

NTNU
Norwegian University of Science and Technology

# Real-time 3-D CFI example

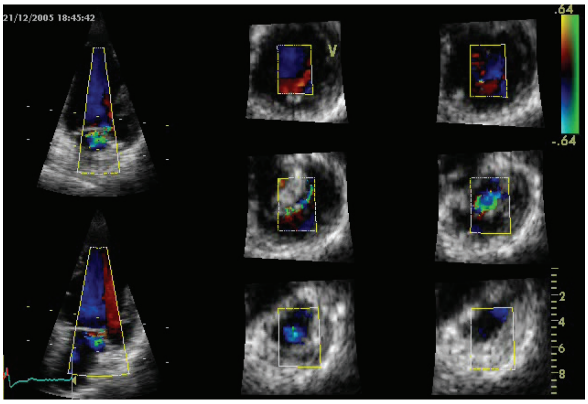


**Example:**

Mitral valve insufficiency

Real-time CFI without ECG triggering and volume stitching

6-slice view – notice the banana shaped leakage in the mitral valve indicated by the green color (increased Doppler bandwidth)

New information!

NTNU
Norwegian University of Science and Technology





# Estimation of Valvular regurgitation Area by 3D HPRF Doppler

Valvular regurgitant jet area can be quantified by isolating the Dopper signal power from the jet over the whole leakage area relative to a known reference signal from the center of the jet (vena contracta)

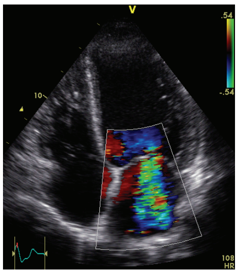

Mitral valve insufficiency

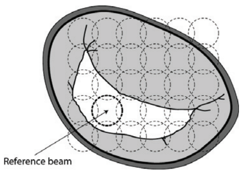


Mitral valve 3-D beam pattern

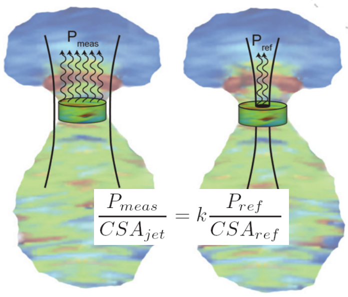

16
3

# In vitro results

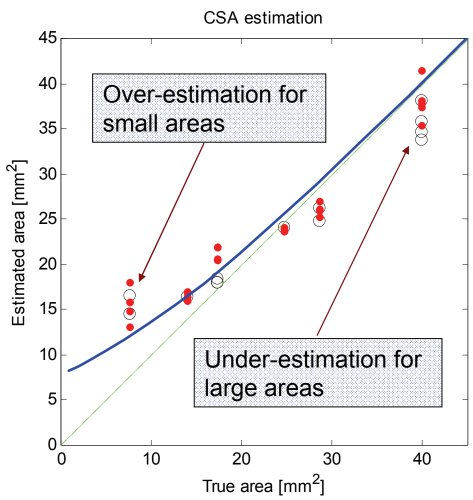


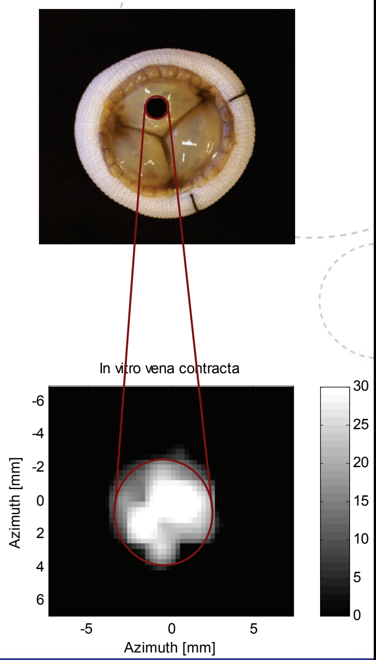




16
4

# In vivo - compared to MRI

- Vena contracta position determined with PW Doppler.
- Jet power isolated with high pulse repetition frequency (HPRF).
- Acquire 3D HPRF data.
- Obtains jet geometry, cross sectional area, and regurgitant volume.
- Small leakages overestimated when compared to MRI. This is expected due to the finite beam width.

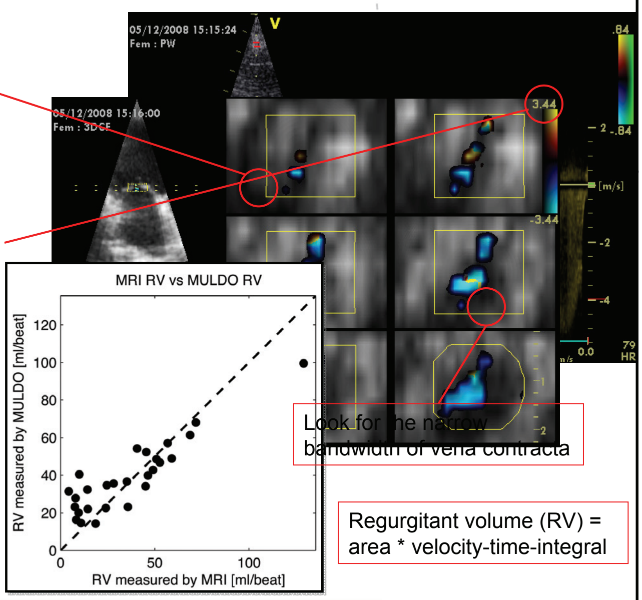

16
5

# Thanks for your attention!

(We hope you enjoyed the show)

**Acknowledgements**
A. Støylen (NTNU), A. Heimdel (GE Vingmed), S. Bjærum (GE Vingmed), K. Kristoffersen (GE Vingmed), T. Hegrum (NTNU), J. Crosby (NTNU), F. Orderud (NTNU), J. Udesen (DTU), J. U. Voigt, S. A. Aase (NTNU), A. Swillens (UGent), P. Segers (UGent), and more…

NTNU
Norwegian University of Science and Technology



16
6

# Reference list

**Textbooks used for all lectures**

1. Angelsen, B.A.J. and H. Torp, *Ultrasound Imaging: Waves, Signals, and Signal Processing*. Vol. 2. 2000, Trondheim: Emantec AS.

2. Doviak, R.J. and D.S. Zrnic, *Doppler RADAR and weather observations*. Second edition ed. 1993, San Diego: Academic press, Inc.

3. Jensen, J.A., *Estimation of Blood Velocities Using Ultrasound*. 1996, New York: Cambridge University Press.

4. Cobbold, R.S.C., *Foundations of Biomedical Ultrasound*. 2007, New York: Oxford University Press, Inc.

NTNU
Norwegian University of Science and Technology

www.ntnu.no H. Torp and L. Lovstakken - Doppler short course '09 - Part I:

167

# Reference list

## PW-Doppler / Color flow imaging


1. Kasai, C., et al., *Real-Time Two-Dimensional Blood Flow Imaging Using an Autocorrelation Technique.* Sonics and Ultrasonics, IEEE Transactions on, 1985. 32(3): p. 458-464.

2. Bonnefous, O. and P. Pesque, *Time domain formulation of pulse-Doppler ultrasound and blood velocity estimation by cross correlation.* Ultrason Imaging, 1986. 8(2): p. 73-85.

3. Kristoffersen, K., *Optimal receiver filtering in pulsed Doppler ultrasound blood velocity measurements.* IEEE Trans Ultrason Ferroelectr Freq Control, 1986. 33(1): p. 51-8.


NTNU
Norwegian University of Science and Technology



168


# Reference list

## PW-Doppler / Color flow imaging



1. Torp, H., K. Kristoffersen, and B.A.J. Angelsen, *Autocorrelation techniques in color flow imaging: signal model and statistical properties of the autocorrelation estimates.* Ultrasonics, Ferroelectrics and Frequency Control, IEEE Transactions on, 1994. 41(5): p. 604-612.

2. Torp, H., X.M. Lai, and K. Kristoffersen. *Comparison between cross-correlation and auto-correlation technique in color flow imaging*. in *Ultrasonics Symposium, 1993. Proceedings., IEEE 1993*. 1993.

3. Torp, H. and K. Kristoffersen, *Velocity matched spectrum analysis: a new method for suppressing velocity ambiguity in pulsed-wave Doppler.* Ultrasound Med Biol, 1995. 21(7): p. 937-44.


NTNU
Norwegian University of Science and Technology

# Reference list

## Clutter filtering

1. Hoeks, A.P., et al., *An efficient algorithm to remove low frequency Doppler signals in digital Doppler systems.* Ultrason Imaging, 1991. 13(2): p. 135-44.

2. Chornoboy, E.S., *Initialization for improved IIR filter performance.* Signal Processing, IEEE Transactions on, 1992. 40(3): p. 543-550.

3. Kadi, A.P. and T. Loupas, *On the performance of regression and step-initialized IIR clutter filters for color Doppler systems in diagnostic medical ultrasound.* Ultrasonics, Ferroelectrics and Frequency Control, IEEE Transactions on, 1995. 42(5): p. 927-937.

4. Torp, H., *Clutter rejection filters in color flow imaging: a theoretical approach.* IEEE Trans Ultrason Ferroelectr Freq Control, 1997. 44(2): p. 417-24.

5. Bjaerum, S. and H. Torp, *Statistical evaluation of clutter filters in color flow imaging.* Ultrasonics, 2000. 38(1-8): p. 376-80.

NTNU
Norwegian University of Science and Technology





# Reference list

## Clutter filtering

1. Bjaerum, S., H. Torp, and K. Kristoffersen, *Clutter filter design for ultrasound color flow imaging.* IEEE Trans Ultrason Ferroelectr Freq Control, 2002. 49(2): p. 204-16.

2. Thomas, L. and A. Hall. *An improved wall filter for flow imaging of low velocity flow*. in *Ultrasonics Symposium, 1994. Proceedings., 1994 IEEE*. 1994.

3. Bjaerum, S., H. Torp, and K. Kristoffersen, *Clutter filters adapted to tissue motion in ultrasound color flow imaging.* IEEE Trans Ultrason Ferroelectr Freq Control, 2002. 49(6): p. 693-704

4. Lovstakken, L., et al., *Real-time adaptive clutter rejection filtering in color flow imaging using power method iterations.* IEEE Trans Ultrason Ferroelectr Freq Control, 2006. 53(9): p. 1597-608.

NTNU
Norwegian University of Science and Technology

17
1

# Reference list


**2-D flow velocity estimation**

1. Scabia, M., et al., *A real-time two-dimensional pulsed-wave Doppler system.* Ultrasound Med Biol, 2000. 26(1): p. 121-31.

2. Dunmire, B., et al., *Cross-beam vector Doppler ultrasound for angle-independent velocity measurements.* Ultrasound Med Biol, 2000. 26(8): p. 1213-35.

3. Anderson, M.E., *Multi-dimensional velocity estimation with ultrasound using spatial quadrature.* IEEE Trans Ultrason Ferroelectr Freq Control, 1998. 45(3): p. 852-61.

4. Jensen, J.A. and P. Munk, *A new method for estimation of velocity vectors.* IEEE Trans Ultrason Ferroelectr Freq Control, 1998. 45(3): p. 837-51.




17
2

# Reference list


**2-D flow velocity estimation**

1. Trahey, G.E., J.W. Allison, and O.T. von Ramm, *Angle independent ultrasonic detection of blood flow.* IEEE Trans Biomed Eng, 1987. 34(12): p. 965-7.

2. Bohs, L.N., et al., *A real time system for quantifying and displaying two-dimensional velocities using ultrasound.* Ultrasound Med Biol, 1993. 19(9): p. 751-61.

3. Friemel, B.H., et al., *Speckle decorrelation due to two-dimensional flow gradients.* IEEE Trans Ultrason Ferroelectr Freq Control, 1998. 45(2): p. 317-27.

4. Bohs, L.N., et al., *Speckle tracking for multi-dimensional flow estimation.* Ultrasonics, 2000. 38(1-8): p. 369-75.

5. Lovstakken, L., et al., Blood flow imaging - A new real-time, 2-D flow imaging technique. IEEE Trans Ultrason Ferroelectr Freq Control, 2006. 53(2): p. 289-99.

17
3

# Reference list


**High frame rate CFI**

1. T. Hergum et al., *Reducing Color Flow Artifacts caused by Parallel Beamforming*, IEEE Trans. Ultrason., Ferrielect. And Freq. Contr. *submitted, 2009*

2. S. I. Nikolov and J. A. Jensen, In-Vivo Synthetic Aperture Flow Imaging in Medical Ultrasound, IEEE Trans. Ultrason., Ferrielect. And Freq. Contr. vol. 50, no. 7, July 2008

3. N. Odderhede et al, Multi-Frequency Encoding for Fast Color Flow or Quadroplex Imaging, IEEE Trans. Ultrason., Ferrielect. And Freq. Contr. vol. 55, no. 4, April 2008


NTNU
Norwegian University of
Science and Technology